REPUBLIC OF TURKEY
YILDIZ TECHNICAL UNIVERSITY
GRADUATE SCHOOL OF NATURAL AND APPLIED SCIENCES

AERODYNAMIC OPTIMIZATION OF DIFFUSER FOR HORIZONTAL AXIS WIND TURBINE

Şafak DOĞRU

MASTER OF SCIENCE THESIS

Department of Naval Architecture and Marine Engineering
Program of Naval Architecture and Marine Engineering

Advisor
Asst. Prof. Dr. Oktay YILMAZ

November, 2019

REPUBLIC OF TURKEY
YILDIZ TECHNICAL UNIVERSITY
GRADUATE SCHOOL OF NATURAL AND APPLIED SCIENCES

AERODYNAMIC OPTIMIZATION OF DIFFUSER FOR HORIZONTAL AXIS WIND TURBINE

A thesis submitted by Şafak DOĞRU in partial fulfillment of the requirements for the degree of **MASTER OF SCIENCE** is approved by the committee on 12.11.2019 in Department of Naval Architecture and Marine Engineering , Program of Naval Architecture and Marine Engineering .

Asst. Prof. Dr. Oktay YILMAZ
Yildiz Technical University
Advisor

Approved By the Examining Committee

Asst. Prof. Dr. Oktay YILMAZ, Advisor
Yildiz Technical University _____

Asst. Prof. Dr. Yasemin ARIKAN ÖZDEN, Member
Yildiz Technical University _____

Assoc. Prof. Dr. Levent KAVURMACIOĞLU, Member
Istanbul Technical University _____

I hereby declare that I have obtained the required legal permissions during data collection and exploitation procedures, that I have made the in-text citations and cited the references properly, that I haven't falsified and/or fabricated research data and results of the study and that I have abided by the principles of the scientific research and ethics during my Thesis Study under the title of Aerodynamic Optimization of Diffuser for Horizontal Axis Wind Turbine supervised by my supervisor, Asst. Prof. Dr. Oktay YILMAZ. In the case of a discovery of false statement, I am to acknowledge any legal consequence.

Şafak DOĞRU

Signature

Dedicated to my family
and my best friends
and a sustainable world

ACKNOWLEDGEMENTS

I would first like to thank my thesis advisor Asst. Prof. Oktay YILMAZ. The door to Asst. Prof. Oktay YILMAZ office was always open whenever I ran into a trouble spot or had a question about my research or writing. He consistently allowed this paper to be my own work, but steered me in the right direction whenever he thought I needed it.

I would like to thank Prof. Lars SÆTRAN and Prof.Per-Åge KROGSTAD who share the open rotor geometry for validation from Department of Energy and Process Engineering at The Norwegian University of Science and Technology.

I would also like to thank the experts who were involved for this research project: My dear manager Uğur AY and my dear colleague Gökhan DEVECİ. Without their passionate participation and input, the research could not have been successfully conducted.

I would like to endless thank my family, who supported me in every subject at every stage of my thesis.

Şafak DOĞRU

TABLE OF CONTENTS

LIST OF SYMBOLS vii

LIST OF ABBREVIATIONS viii

LIST OF FIGURES ix

LIST OF TABLES xi

ABSTRACT xii

ÖZET xiv

1 Introduction 1
- 1.1 Literature Review . . . 1
- 1.2 Objective of the Thesis . . . 5
- 1.3 Hypothesis . . . 5

2 Wind Turbine 6
- 2.1 Wind Energy . . . 6
- 2.2 Wind Turbine . . . 6
  - 2.2.1 Wind Electricity Generation in the World . . . 6
  - 2.2.2 Fundamental Components of the Horizontal Axis Wind Turbine 9
  - 2.2.3 History of the Wind Turbine . . . 13
- 2.3 Efficiency in Wind Turbines and Betz Limit . . . 19

3 Computational Fluid Dynamics(CFD) 20
- 3.1 Determination of the Purpose of the Analysis . . . 21
- 3.2 Creation and Preparation Geometry for Calculation . . . 22
- 3.3 Generation of Mesh . . . 22
  - 3.3.1 Governing Equations of the Flow . . . 24
  - 3.3.2 Turbulence Modelling . . . 24
  - 3.3.3 Moving Reference Frame . . . 25
- 3.4 Definition of Required Physics and Boundary Conditions . . . 27
- 3.5 Solution . . . 27

3.6 Post-processing 27

4 Methods **28**
4.1 Validation 28
4.2 Optimization 34
4.2.1 Preparation of Parametric Geometry 37
4.2.2 Response Surface Optimization 37
4.3 Rotor with diffuser 42

5 Results of Optimized Diffuser for Horizontal Axis Wind Turbine **43**
5.1 Rotating Diffuser 43
5.2 Stationary Diffuser 44

6 Conclusions **51**

A Ansys SpaceClaim Direct Modeller Python Script **52**

References **57**

Publications From the Thesis **60**

LIST OF SYMBOLS

α	Angle of attack
Ω	Angular Velocity
$^{\circ}$	Degrees
ρ	Density
μ	Dynamic viscosity
U_{∞}	Freestream velocity
υ	Kinematic viscosity
C_p	Power Coefficient
$C_p^{'}$	Pressure Coefficient
rpm	Revolutions per minute
C_T	Thrust Coefficient
u, v, w	Velocity vectors

LIST OF ABBREVIATIONS

CCD	Central Composite Design
CAD	Computer Aided Design
CFD	Computational Fluid Dynamics
HAWT	Horizontal Axis Wind Turbine
k-ω	K-omega Turbulence Model
MRF	Moving Eeference Frame
RANS	Reynolds Averaged Navier Stokes
SST	Shear Stress Transport
SCDM	SpaceClaim Direct Modeller
TSR	Tip Speed Ratio
VAWT	Vertical Axis Wind Turbine

LIST OF FIGURES

Figure 1.1 Power coefficient of the model turbine in [17] 3
Figure 1.2 Thurst coefficient of the model turbine in [17] 4
Figure 2.1 Top 10 countries with the highest installed power onshore wind power in 2018 and other countries 7
Figure 2.2 Top 10 countries with the highest new installations onshore wind power in 2018 and other countries 7
Figure 2.3 Top 10 countries with the highest installed power offshore wind power in 2018 and other countries 8
Figure 2.4 Top 10 countries with the highest new installations offshore wind power in 2018 and other countries 8
Figure 2.5 Fundamental components of the wind turbine [19] 10
Figure 2.6 Heron's machine of water wheel [20] 13
Figure 2.7 Some examples of wind wheels of grinding flour and pumping water in the history 14
Figure 2.8 Chance aground at Bluff in 1902 [25] 15
Figure 2.9 Beginning of the renewable wind energy for electricity [26] 15
Figure 2.10 Design of Darrieus wind turbine [27] 16
Figure 2.11 NASA experimental wind turbines [29] 16
Figure 2.12 The wind turbine at Tvind [30] 17
Figure 2.13 Evolution of the wind turbines [31] 17
Figure 2.14 Growth of onshore and offshore wind turbines [32] 18
Figure 3.1 The structure of a mesh 23
Figure 3.2 Element types of mesh 23
Figure 3.3 Vector transformations between moving and stationary frames [34] 25
Figure 4.1 Flow volume of validation geometry 29
Figure 4.2 The Image of MRF geometry 30
Figure 4.3 The image of the mesh-1 ($y^+ \approx 1$) 31
Figure 4.4 The image of the mesh-2 ($y^+ \approx 1$) 31
Figure 4.5 Mesh independence study in CFD for Open Rotor Turbine 32
Figure 4.6 Comparisons of power coefficients from CFD with the measurements 33
Figure 4.7 Comparisons of thrust coefficients from CFD with the measurements 33

Figure 4.8 2D Axisymmetric swirl model and mesh 35
Figure 4.9 Near wall mesh resolution ($y^+ \approx 1$) 35
Figure 4.10 Mesh independence for diffuser optimization 36
Figure 4.11 Inscribed composite design method factor space 38
Figure 4.12 Circumscribed composite design method factor space 39
Figure 4.13 Face centered composite design method factor space 39
Figure 4.14 Response surface of mass flow rate 41
Figure 4.15 Response surface of uniformity of velocity 41
Figure 4.16 Optimal geometry and velocity contour 42
Figure 5.1 Rotating Diffuser 43
Figure 5.2 Comparisons of power coefficients of "Open Rotor" and "Rotor with Diffuser" 44
Figure 5.3 Comparisons of thrust coefficients of "Open Rotor" and "Rotor with Diffuser" 44
Figure 5.4 Comparisons of velocities of "Open Rotor" and "Rotor with Diffuser" in longitudinal plane 45
Figure 5.5 Comparisons of streamwise wind velocity distribution on the rotation axis of wind turbine at TSR=6 46
Figure 5.6 Comparisons of radial wind velocity distribution on front section of wind turbine at TSR=6 46
Figure 5.7 Comparisons of radial wind velocity distribution on rear section of wind turbine at TSR=6 47
Figure 5.8 Sections of blade 47
Figure 5.9 Pressure coefficient distributions along section of blade at r/R=0.2 and TSR=6 48
Figure 5.10 Pressure coefficient distributions along section of blade at r/R=0.4 and TSR=6 48
Figure 5.11 Pressure coefficient distributions along section of blade at r/R=0.6 and TSR=6 49
Figure 5.12 Pressure coefficient distributions along section of blade at r/R=0.8 and TSR=6 49

LIST OF TABLES

Table 4.1 Mesh independence cases information for Open Rotor Turbine . . . 32
Table 4.2 Mesh independence cases information for diffuser optimization . . . 36
Table 4.3 Optimization conditions and objectives 37
Table 4.4 Optimization results of parameters 42
Table 5.1 Optimization conditions and objectives 45

ABSTRACT

Aerodynamic Optimization of Diffuser for Horizontal Axis Wind Turbine

Şafak DOĞRU

Department of Naval Architecture and Marine Engineering
Master of Science Thesis

Advisor: Asst. Prof. Dr. Oktay YILMAZ

Energy costs are increasing, and environmental pollution is becoming more and more serious all over the world. Consequently, there has been a trend towards renewable energy sources. The use of wind energy, which is a renewable energy source, has gained more importance in recent years. As a result, wind turbine systems, one of the wind power electricity generation techniques, have evolved rapidly in the last few decades. This research focused on improving the performance of an experimentally validated conventional three blade horizontal axis wind turbine with an optimum diffuser. In order to understand performance augmentation effects of a diffuser on the wind turbine, the effects of the diffuser shape on the increased wind speed and flow uniformity just around the turbine rotor were investigated by computational fluid dynamics (CFD) analyses. The diffuser is shaped based on GOE431 airfoil. The numerical results have shown that flow uniformity and the wind speed through the diffuser was greatly influenced by the chord length and angle of attack of the airfoil used. The design of diffuser is investigated with the response surface optimization method for maximum wind speed with good flow uniformity around the rotor. In this study, an optimum diffuser augmented wind turbine with power coefficient well beyond the Betz Limit has been developed for a conventional horizontal axis wind turbine with a rotor diameter of 0.90 m.

Keywords: Wind Turbine, CFD, Response Surface Optimization, Diffuser, Betz Limit

YILDIZ TECHNICAL UNIVERSITY
GRADUATE SCHOOL OF NATURAL AND APPLIED SCIENCES

ÖZET

Yatay Eksenli Rüzgar Türbini İçin Difüzörün Aerodinamik Optimizasyonu

Şafak DOĞRU

Gemi İnşaatı ve Gemi Makinaları Mühendisliği Anabilim Dalı
Yüksek Lisans Tezi

Danışman: Dr.Öğr.Üyesi Oktay YILMAZ

Enerji maliyetleri artmakta ve tüm dünyada çevre kirliliği giderek daha ciddi hale gelmektedir. Buna bağlı olarak, yenilenebilir enerji kaynaklarının daha fazla kullanımına başlanmıştır. Yenilenebilir bir enerji kaynağı biri olan rüzgar enerjisinin kullanımı son yıllarda daha fazla önem kazanmıştır. Sonuç olarak, rüzgar enerjisi elektrik üretim tekniklerinden biri olan rüzgar türbini sistemleri, son yıllarda hızla gelişmiştir. Bu araştırmada, deneysel olarak test edilmiş geleneksel üç kanatlı yatay eksenli rüzgar türbininin optimum bir difüzörle performansını arttırmak amaçlanmıştır. Bir difüzörün rüzgar türbini üzerindeki performans artırma etkilerini anlamak için, difüzör şeklinin türbin rotorunun etrafındaki yüksek rüzgar hızı ve akış üniformluğu üzerindeki etkileri hesaplamalı akışkanlar dinamiği (HAD) analizleriyle incelenmiştir. Difüzör GOE431 kanadına göre şekillendirilmiştir. Sayısal sonuçlar, akış üniformluğunun ve difüzör içerisindeki rüzgar hızının, kullanılan kanat kiriş kord uzunluğu ve hücum açısından büyük ölçüde etkilendiğini göstermiştir. Difüzör tasarımı, rotor çevresinde iyi akış homojenliği ile maksimum rüzgar hızı için amaç yüzey optimizasyon yöntemi ile incelenmiştir. Bu çalışmada, 0,90 m'lik bir rotor çapına sahip geleneksel bir yatay eksenli rüzgar türbini için Betz sınırının çok ötesinde bir güç katsayısına sahip difüzörlü rüzgar türbini geliştirilmiştir.

Anahtar Kelimeler: Rüzgar Türbini, HAD, Tepki Yüzey Optimizasyonu, Difüzör, Betz Sınırı

YILDIZ TEKNİK ÜNİVERSİTESİ
FEN BİLİMLERİ ENSTİTÜSÜ

1
Introduction

The world needs a revolution. Sustainability is one of the strategic areas in terms of energy demand increase in parallel with the rapid development of the economy and industry. Ensuring safe and sustainable energy supply worldwide has a direct impact on economic development. Energy demand is expected to be met intensively from fossil fuels in the near future, and it is estimated that the importance of coal and natural gas will continue in the long term and that the importance of nuclear will not decrease despite the recent history accidents. The very low level of energy efficiency increases energy costs, which is the biggest input for both industry and individual users. As a natural result of the intensive consumption of fossil resources, the ecological balance has been adversely affected. Minimizing carbon emissions per capita will ensure the continuity of a sustainable world to save our future.

Many countries worldwide use wind turbines to generate electricity through renewable energy sources and use this environmentally friendly system. Due to the increase in energy demand and population growth in the world, the use of wind energy, which is one of the leading renewable energy sources, has gained more significance in recent years.

1.1 Literature Review

Among the renewable energy sources, the most popular issue in the world for the time being is the efforts to make maximum use of wind energy. The main reason for this is that the wind is an easily accessible source. Researches, PhD theses and graduation projects are increasing in number on the usability of the existing systems at maximum level and bringing differences with the innovation work. There exist lots of studies concentrated on wind turbine with diffuser [1–4]. Productivity, portability, ease of use and minimum cost can be considered to be advantages of wind energy renewable energy systems. When we consider these systems, electrical energy from wind prevents pollution in the atmosphere with zero carbon emission. With increasing

use of wind energy and increasing interest in renewable energy in the world, the number of wind energy systems increased. In particular, numerical investigations have been carried out for the flow areas around flanged diffusers to develop small wind turbines by Phillips et al. [3] and Abe and Ohya [4]. Hansen et al. [5] showed that the increase in mass flow in the area where the wind turbine is located is very important, and "Betz limit" can be exceeded.

Computational fluid dynamics (CFD) methods are very effective in determining the performance of wind turbines [6]. Flow, heat transfer, mass transfer and many user-definable scenarios can be modeled with the modern CFD codes used today and in the past [7].

Saha et al. and Altan et al. studied experimentally the three-dimensional displacement on the rotary blade. They have mentioned about the importance of non-contact and full motion measurements in rotating objects in engineering. Experimental results showed that the proposed system's rotating blade measurements can be performed in three dimensions. The results of this experiment showed that this method can be used to design a wind turbine [8, 9].

In Wu et al. and Winstroth et al. the three-dimensional imaging system was examined in three-dimensional displacement of the entire field using a pair of synchronized high-speed cameras. With this system, applied measurement of three dimensional displacement of wind turbine model at multiple speeds has been made [10, 11].

In order to examine experimentally a physically identical wind turbine in the laboratory conditions, Kelberlau examined the use of a turbine 40 times smaller than the original turbine. Using similarity methods, Kelberlau investigated the importance and efficiency of scaling in the evaluation and performance analysis of wind turbines [12].

In general, RANS is used in computational fluid dynamics simulations. $K-\omega$ models are one of the most common turbulence models used in engineering designs. This model is numerically easy to converge, and it emerges as a computationally low cost model [13]. Menter et al. explained the SST turbulence model.

To help understanding the flow characteristics around the wind turbine 3 (three) dimensional turbulence is necessary to consider to clarify the flow field variables. In such cases, CFD software is used to determine turbulence field variables. In the study carried out by Mandas et al., the use of the $k-\omega$ turbulence model showed good results in the calculation of axial velocities [14].

The study conducted by the aerodynamic design and improvement methodology has been carried out by Fuglsang and Madsen. Optimization studies in the study have become an important step for horizontal axis wind turbine development [15]. Understanding the relationship between geometric and output parameters is very important for wind turbine designs. As the number of parameters increases, understanding these relationships requires a costly and time-consuming process. In modern engineering, response surface method has become a good tool for a better understanding of all relations [16].

In the study of Krogstad and Adaramola [17], a three-bladed horizontal axis wind turbine model with an upstream rotor of 0.90 m diameter is investigated. In the study, turbine power properties was obtained at different freestream velocities experimentally. The turbine power characteristics of the study can be seen in Figure 2.15 and Figure 2.16.

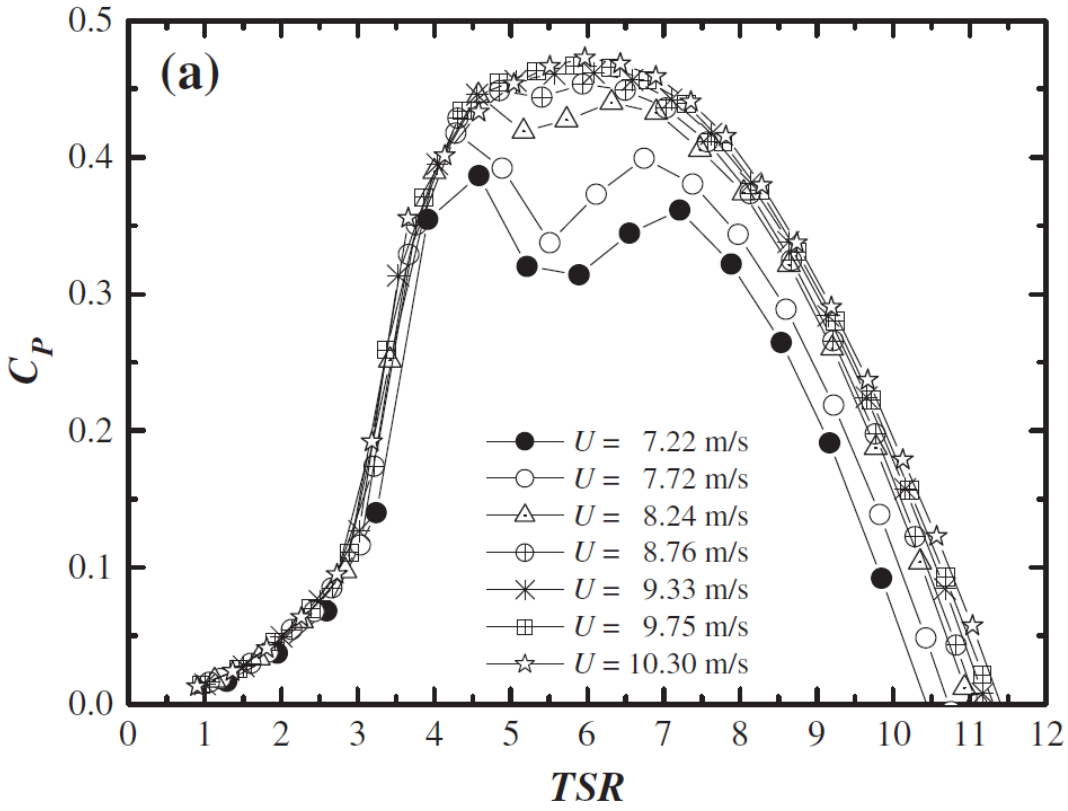

Figure 1.1 Power coefficient of the model turbine in [17]

Also, in this study, the wind turbine geometry is the same as Krogstad and Adaramola [17] for validation step. As can be understood from the literature review, small horizontal axis wind turbine can properly be used with diffuser.

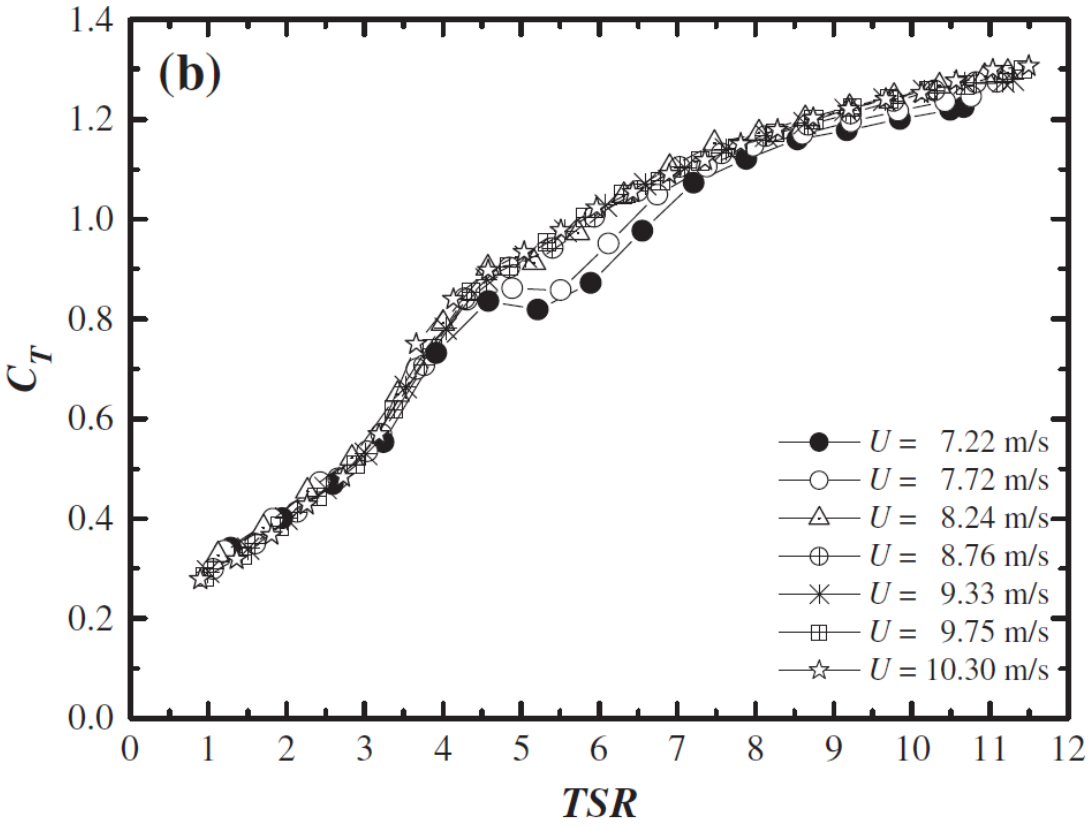

Figure 1.2 Thurst coefficient of the model turbine in [17]

1.2 Objective of the Thesis

In this study, validation studies are performed with CFD for a wind turbine [17] that was examined experimentally before. Using the k-ω turbulence model, three dimensional computational fluid dynamics (CFD) simulations are performed and numerical calculations are performed. In the second part of the study, the optimum design point is determined by using response surface optimization method for the operation of the wind turbine with a diffuser. Design variables (angle of attack and chord length of the airfoil) for the diffuser are optimized for maximum mass flow of air with as uniform wind speed as possible in this stage. Analyzes are performed for the rotating and stationary diffuser with the optimized diffuser geometry.

1.3 Hypothesis

The goal of this study is to investigate the effect of rotating and stationary diffuser on turbine performance compared to the open rotor geometry.

2
Wind Turbine

2.1 Wind Energy

Wind energy is one of the important renewable and inexhaustible types of energy that does not cause pollution. Increasing global climate change and concerns about energy security, wind energy have placed at the center of the new economical development strategies. Unlike conventional energy sources, wind energy does not cause greenhouse gas release.

2.2 Wind Turbine

Wind turbines generate electrical energy by utilizing wind energy. Wind turbines are the main structural elements of wind power plant. The system that first converts the kinetic energy of the flowing air into mechanical energy. Then mechanical energy converts into electrical energy. Wind turbines are produced with horizontal axis and vertical axis according to which direction the rotation axis rotates. Horizontal axis wind turbines(HAWT) are the most commonly used of these types, and rotation axes are parallel to the direction of the wind, and the blades operate perpendicular to the wind direction. This type of wind turbines are made of one, two, three or multiple blades.

2.2.1 Wind Electricity Generation in the World

In recent years, wind energy is one of the most utilized renewable energy sources in the world. As of the end of 2018, the total installed wind power in the world is 591,549 MW. 23,14 MW of this power has offshore wind installed power [18].

In April 2019, Global Wind Energy Council (GWEC) published the Global Wind Report. According to this report, China, United States, Germany, India, Brazil, France, Mexico, Sweden, United Kingdom and Canada are the top 10 countries that invested in onshore wind power in 2018, respectively. Respectively China, United States, Germany, India,

Brazil, France, Mexico, Sweden, United Kingdom and Canada are the top 10 countries that have installed onshore wind power until the end of 2018. These data are presented in Figure 2.1 and Figure 2.2 [18].

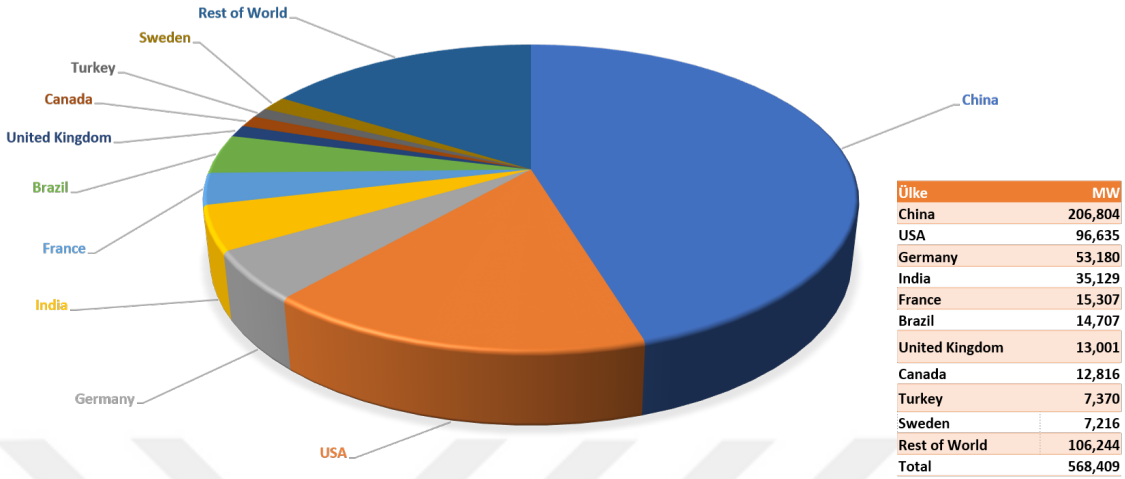

Ülke	MW
China	206,804
USA	96,635
Germany	53,180
India	35,129
France	15,307
Brazil	14,707
United Kingdom	13,001
Canada	12,816
Turkey	7,370
Sweden	7,216
Rest of World	106,244
Total	568,409

Figure 2.1 Top 10 countries with the highest installed power onshore wind power in 2018 and other countries

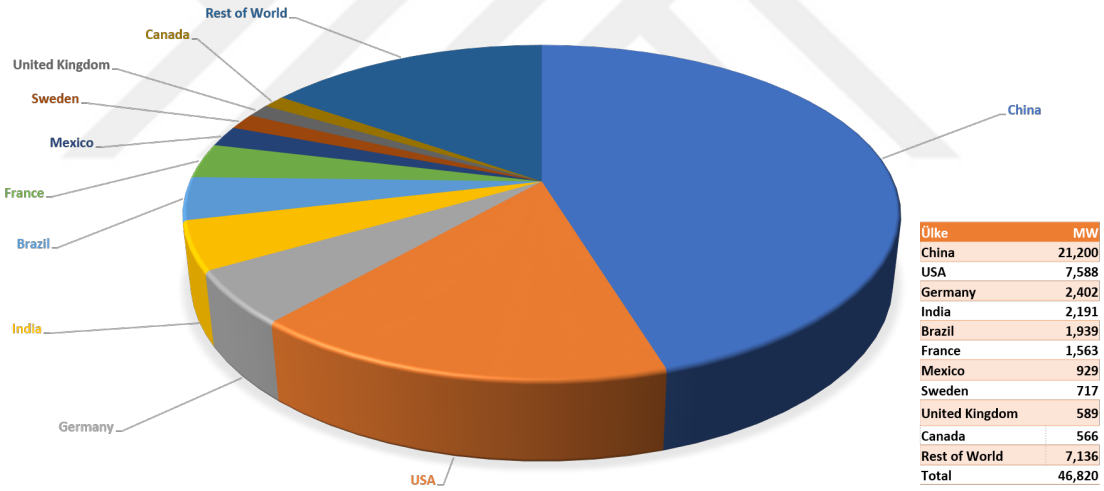

Ülke	MW
China	21,200
USA	7,588
Germany	2,402
India	2,191
Brazil	1,939
France	1,563
Mexico	929
Sweden	717
United Kingdom	589
Canada	566
Rest of World	7,136
Total	46,820

Figure 2.2 Top 10 countries with the highest new installations onshore wind power in 2018 and other countries

According to the report, respectively China, United Kingdom, Germany, Belgium and Denmark are the top 5 countries that invested in offshore wind power in 2018. Respectively United Kingdom, Germany, China, Denmark and Belgium are the top 5 countries that installed onshore wind power until the end of 2018. These data are presented in Figure 2.3 and Figure 2.4 [18].

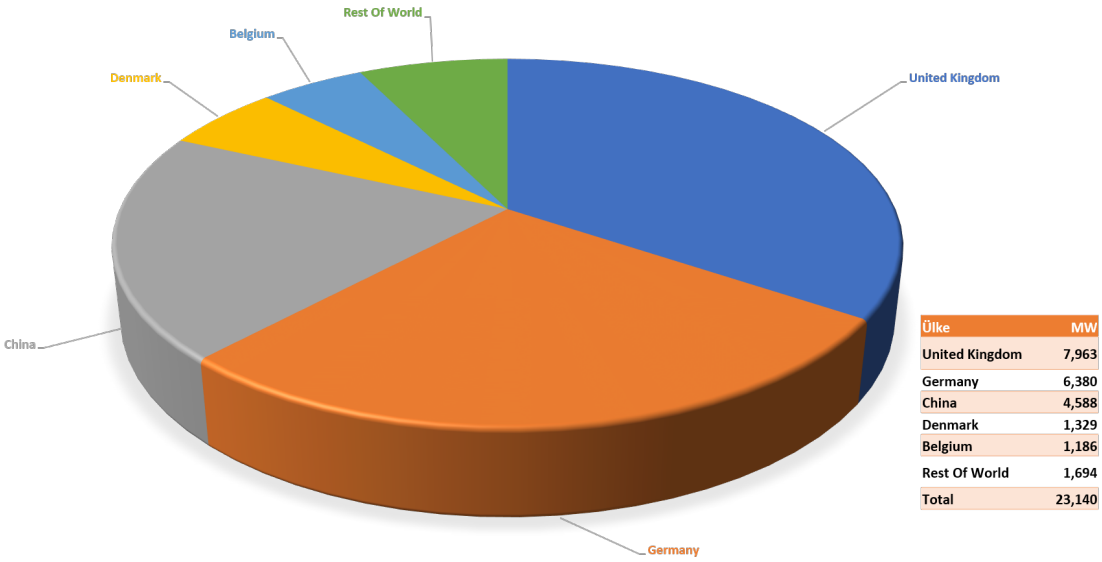

Ülke	MW
United Kingdom	7,963
Germany	6,380
China	4,588
Denmark	1,329
Belgium	1,186
Rest Of World	1,694
Total	23,140

Figure 2.3 Top 10 countries with the highest installed power offshore wind power in 2018 and other countries

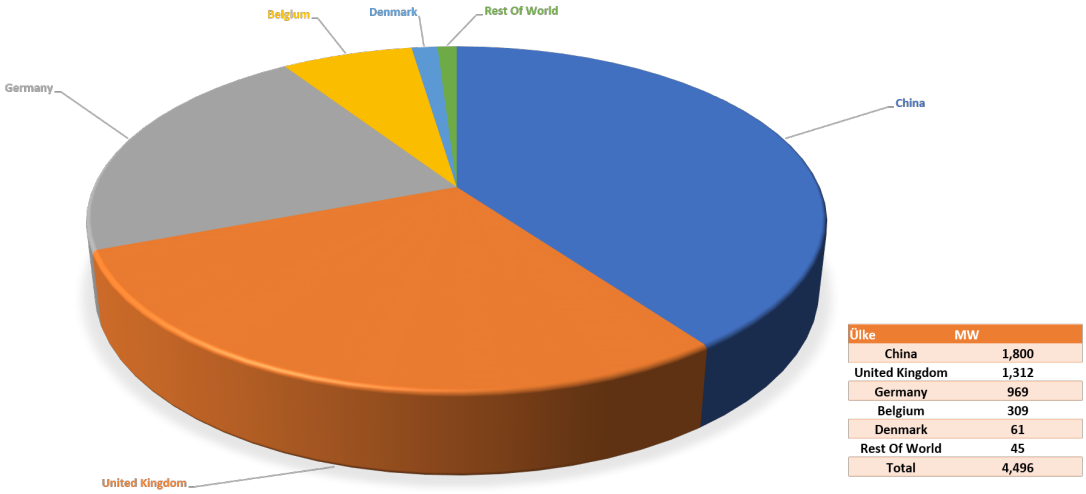

Ülke	MW
China	1,800
United Kingdom	1,312
Germany	969
Belgium	309
Denmark	61
Rest Of World	45
Total	4,496

Figure 2.4 Top 10 countries with the highest new installations offshore wind power in 2018 and other countries

2.2.2 Fundamental Components of the Horizontal Axis Wind Turbine

A wind turbine is formed by connecting a rotor, a nacelle and a tower and several blades mechanically to the generator. The kinetic energy of wind power is converted into mechanical energy by the rotor of the wind turbine. The mechanical gearbox converts the rotational speeds of the rotor to higher speeds in the generator. The electrical energy supplied by the generator is stored in the batteries or transmitted directly to the receivers. The power output generated by the rotation of the generator shaft is provided by a control system.

You can find the fundamental components of the wind turbine in Figure 2.5 and descriptions below.

- Anemometer
- Blades
- Brake
- Controller
- Gearbox
- Generator
- Low speed shaft
- High speed shaft
- Nacelle
- Pitch system
- Rotor
- Tower
- Wind direction
- Wind vane
- Yaw drive
- Yaw motor

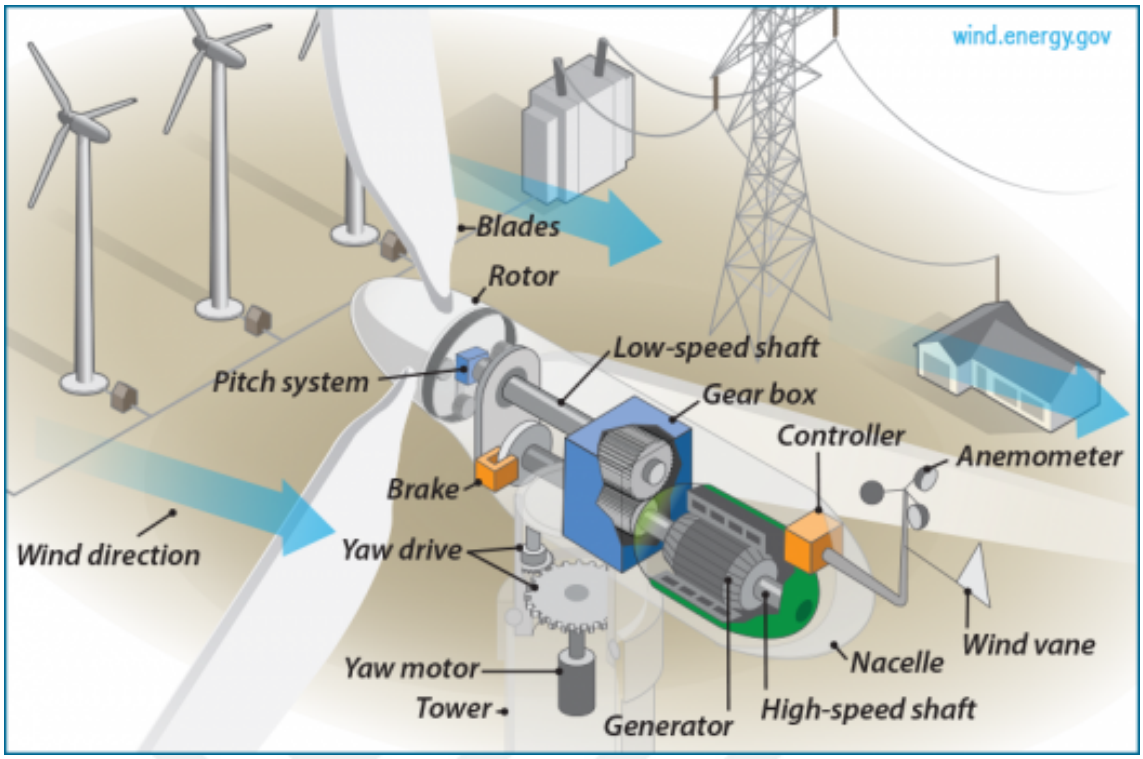

Figure 2.5 Fundamental components of the wind turbine [19]

2.2.2.1 Anemometer

It is used to measure the air velocity and direction of the wind. When the wind speed reaches a certain level, the signal data transmitted by the anemometer by the computer control section of the turbine is used to ensure the movement of the blades. For example, when the wind speed in general exceeds 25 m/s, the control unit automatically stops the turbine operation to prevent damage to the turbine. The speed controller determines the speed range of the turbine. The speed controller determines the cut-in speed at which the wind turbine will take action and the cut-out speed at which the turbine will stop operating.

2.2.2.2 Blades

The turbine blades catch the wind and transfer the mechanical work done by rotational movement to the generator via the shafts. Turbine blades are generally made of composite materials. In addition, the blades are designed to be able to move around its own axis 90° to increase the efficiency from the wind.

2.2.2.3 Brake

Brakes are used for slowing, stopping and holding the turbine's rotors, including emergency stops.

2.2.2.4 Controller

The controller incorporates a computer system that constantly monitors the operation of the wind turbine and performs pitch angle control. In case of any malfunction, for example overheating of the generator or gear system, it ensures that the turbine system stops automatically and sends information about the event by sending signals to the turbine operator. This system enables the turbine to be deactivated.

2.2.2.5 Gearbox

Connects the low-speed shaft to the high-speed shaft and increases the rotational speeds from about 30-60 rotations per minute (rpm) to about 1,000-1,800 rpm. This is the rotational speed required for most generators to generate electricity. The gearbox is an expensive part of the wind turbine, and researchers are investigating "direct drive" generators that operate at low rotational speeds, and do not require gearboxes [19].

2.2.2.6 Generator

Generator converts mechanical energy into electrical energy. It has a system similar to an electric motor and has magnets inside. In the middle of this magnet there is a section wrapped with fine wires. With the rotation of the wings, the mechanical work here becomes electrical energy. Generators are composed of two groups as synchronous or asynchronous motors.

2.2.2.7 Low speed shaft

The low speed shaft of the wind turbine connects the impeller hub to the gearbox.

2.2.2.8 High speed shaft

The wind-driven rotor is on a low-speed shaft which is connected by gears to the high-speed shaft, and it drives the generator.

2.2.2.9 Nacelle

In this part, the wind turbine contains the parts including the gear box, generator, brake system, shafts and protects against external factors. Service personnel can enter this place from the turbine tower. At the front of the machine section, the wind turbine has blades, flanges and nose.

2.2.2.10 Pitch system

With pitch control, the wind turbine blades rotate axially to determine the direction of the wind, and then to the direction of the wind with the entire turbine pitch mechanism.

2.2.2.11 Rotor

The rotor consists of a hub connected to the blades and the housing. The wings catch the wind and transfer power to the core. The rotor is connected to the shaft by a hub and the hub is connected to the low speed shaft of the turbine. With the rotation of the blades, one end rotates the shaft connected to the hub and the other end connected to the generator. The rotor rotation is controlled perpendicular to the wind direction.

2.2.2.12 Tower

The tower is a system component that directly affects wind power and electricity generation. As is known, wind speed and energy are directly proportional to height. Therefore, the higher the tower length, the more energy is produced. Of course, the high tower means more cost and varies according to the field conditions. The towers may be circular or square shaped according to their design. The most important advantage of the square towers is that they have a lower budget in terms of cost. Circle-shaped towers, stairs to reach the turbine nacelle part of the ground is generally made of concrete and steel structure of the tower. One of the most important parameters affecting the construction of the tower is the bending frequency, so the robustness of the tower is very important. In fact, the cost of the wind turbine up to 20% is the construction of the tower.

2.2.2.13 Wind direction

Determines the design of the turbine. Wind flows from rear for downwind type turbines, and wind flows from front for upwind type turbines. [19].

2.2.2.14 Wind vane

The signals are used by the electronic control unit of the wind turbine to rotate the wind turbine against the wind.

2.2.2.15 Yaw drive

The wind is always blowing from one direction and can blow in many different directions during the year. Wind turbines also have blades and mechanisms that rotate the entire turbine to the wind direction for maximum electricity generation. It is operated by an electronic controller that determines the direction of the wind.

2.2.2.16 Yaw motor

Uses electric motors to rotate the rotor towards the wind.

2.2.3 History of the Wind Turbine

The power of the wind has attracted the attention of mankind thousands of years ago. The wind was first used to propulsion of sailing ships. The first wind wheel belongs to Heron of Alexandria, and Heron's machine of water wheel can be found in Figure 2.6 according to Schmidt [20].

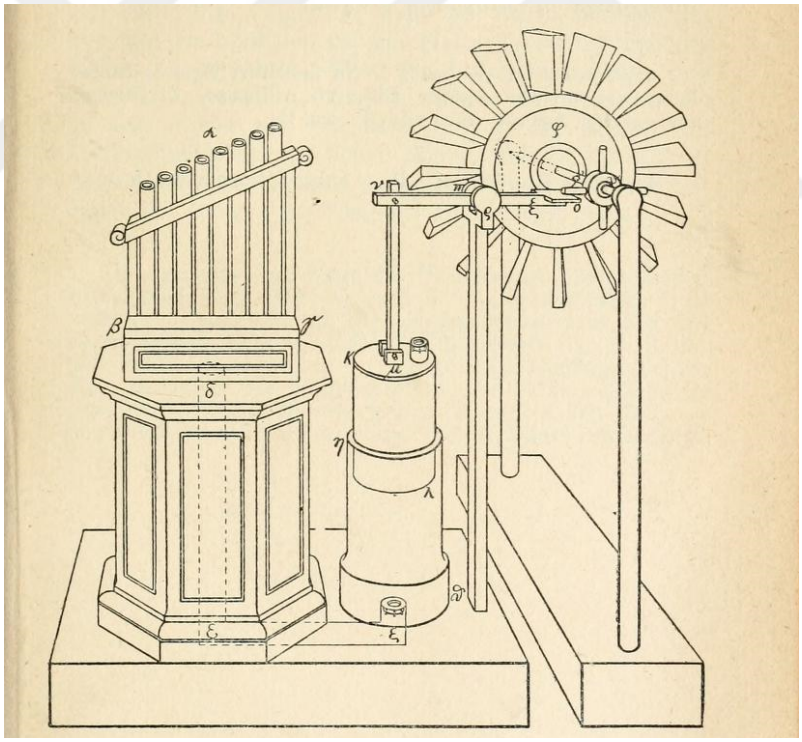

Figure 2.6 Heron's machine of water wheel [20]

During history wind wheels has been used to grind flour and pump water until the end of 19th century in the world. Some examples can be found in the Figure 2.7.

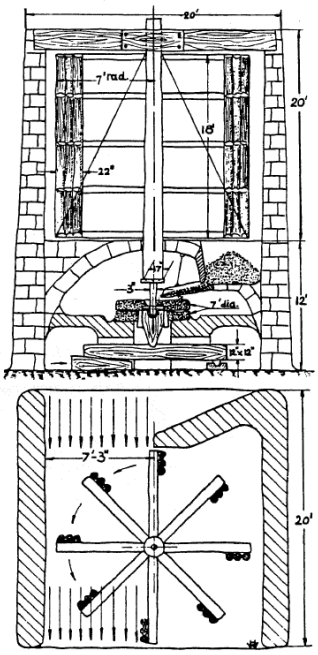

(a) Persian type wind wheels [21]



(b) A windmill in Wales, 1815 [22]

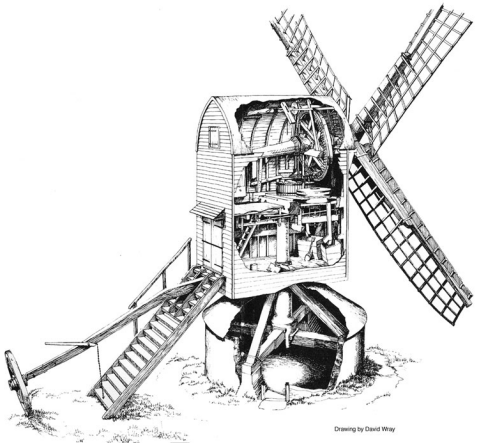

(c) European post-mill, designed to rotate as a whole to face the wind [23]



(d) 14th Century Windmill [24]

Figure 2.7 Some examples of wind wheels of grinding flour and pumping water in the history

In the Figure 2.8, after 100 years of use, in 1902, a ship named Chance can be seen as aground. There is an electric generator using the wind source on board.



Figure 2.8 Chance aground at Bluff in 1902 [25]

The first wind turbine was built in Scotland in 1887 by James Blyth. Blyth's wind turbine is the beginning of the production of wind energy for electricity. It can be found in the Figure 2.9 [26].

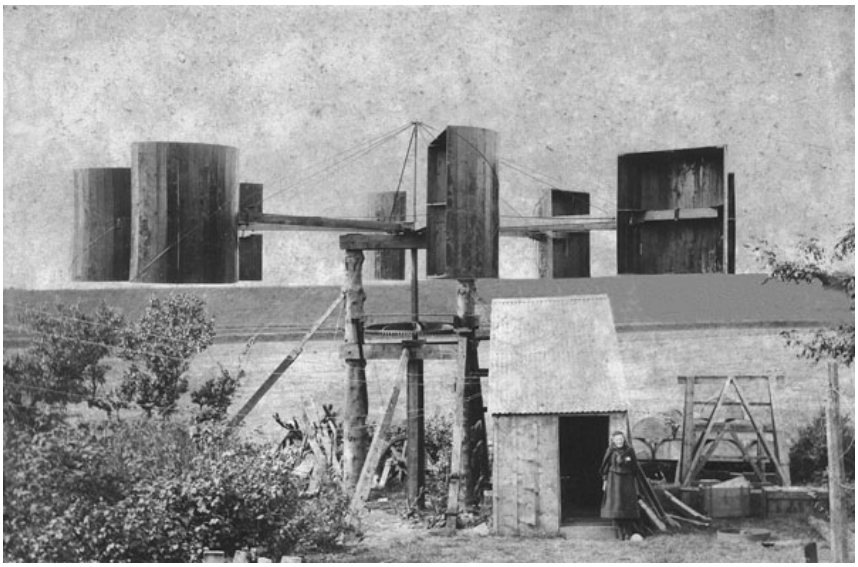

Figure 2.9 Beginning of the renewable wind energy for electricity [26]

The development of modern wind turbines used for production of electricity has began in the 20th century. Until the oil crisis in 1973, the use of wind turbines was generally individual for small capacity farms.

Designs of vertical axis wind turbine and horizontal axis wind turbine are improved. Usually this developments are about system efficiencies and high number megawatts. One of example for vertical axis wind turbine(VAWT) is the Darrieus wind turbine [27]. Design of Darrieus wind turbine can be found in Figure 2.10. Also the world's first megawatt wind turbine is a horizontal axis wind turbine which is Smith-Putnam wind turbine, and it is design by Palmer Cosslett Putnam in 1941 [28].

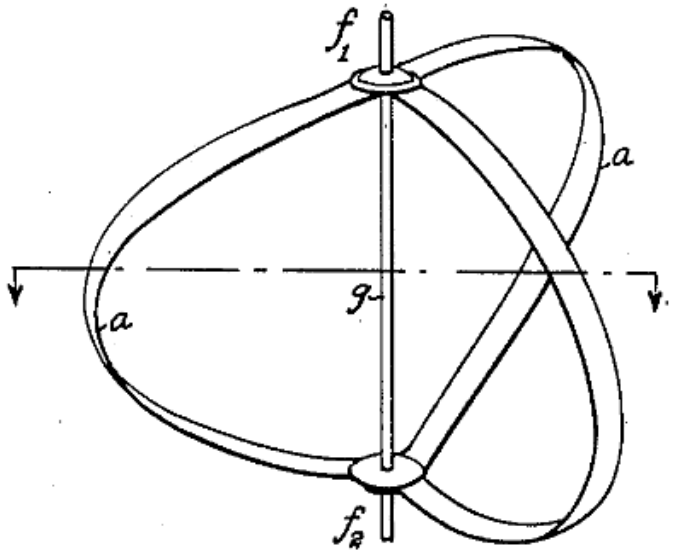

Figure 2.10 Design of Darrieus wind turbine [27]

After the 1973 oil crisis, trends of governments improved the use of wind turbines. Especially, in United States of America, NASA wind turbines has been developed with funding programs between 1973 to 1988. These turbines can be found below in Figure 2.11 [29].

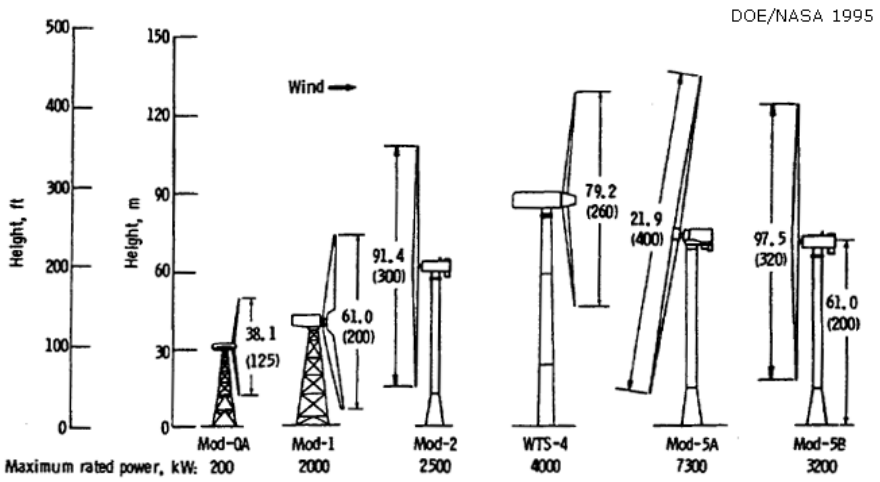

Figure 2.11 NASA experimental wind turbines [29]

Tvindkraft is the first multi-megawatt wind turbine in the world, and it started producing electricity on the 26th of March 1978 in Denmark [30]. The turbine can be seen in Figure 2.12.



Figure 2.12 The wind turbine at Tvind [30]

With time, wind turbines evolved into modern wind turbines of today. The evolution of the wind turbines from 1980 to 2010 can be examined in the Figure 2.13 according to rotor diameter and power capacity [31].

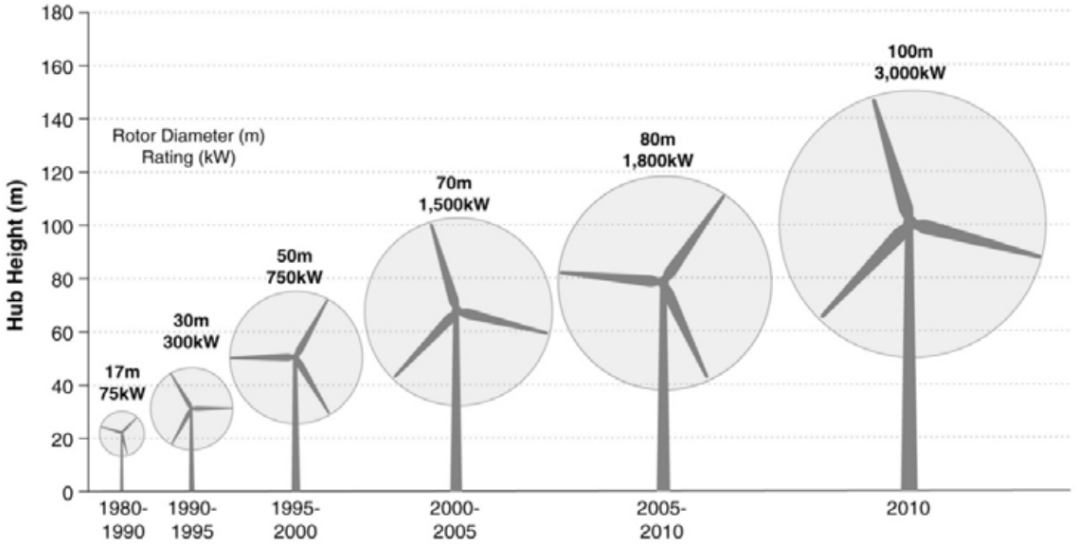

Figure 2.13 Evolution of the wind turbines [31]

In addition, the size offshore wind turbines grown and the weight lightened over the years [32]. Offshore wind turbines and onshore wind turbines comparison can be found in Figure 2.14.

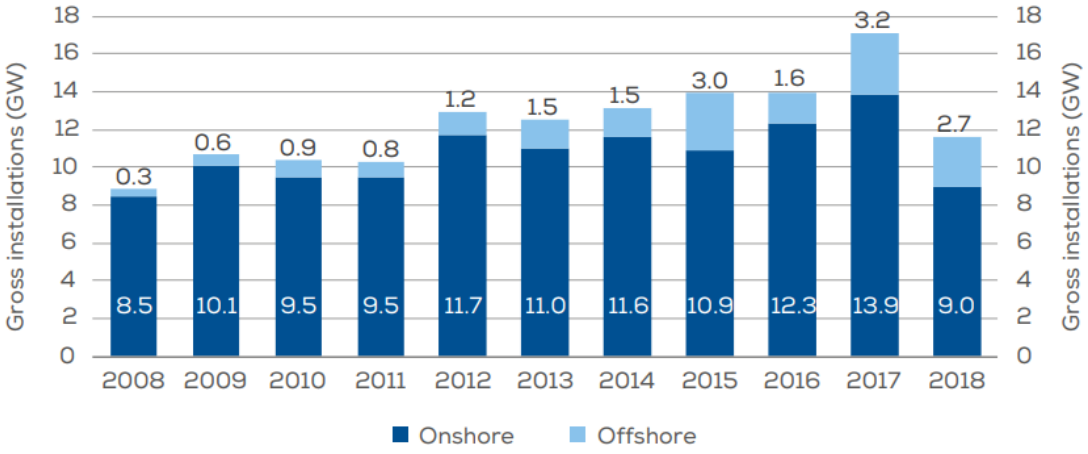

Figure 2.14 Growth of onshore and offshore wind turbines [32]

2.3 Efficiency in Wind Turbines and Betz Limit

The first theory of wind turbines was presented in 1926 at the Göttingen Institute. It was proposed by Albert Betz. In this theorem, the Betz wind rotor is assumed to be ideal. In other words, the rotor consists of an infinite number of wings which do not exhibit drift resistance to air. In this way, it is assumed that the wind rotor is an excellent energy converter [33].

Power coefficient and thrust coefficient can be found below.

$$C_p = \frac{2T\Omega}{\rho \pi R^2 U_\infty^3} \tag{2.1}$$

Where T is torque, and torque is generated by rotor. Ω is rotor angular speed, ρ is density of air, R is radius of rotor, U_∞ is freestream velocity of air.

$$C_T = \frac{2D}{\rho \pi R^2 U_\infty^2} \tag{2.2}$$

Where D is drag force.

Under ideal conditions, theoretically we can convert 59.3% of the kinetic energy in the blowing air into mechanical energy. In other words, theoretically power coefficient equals "16/27", and it is described as Betz Limit. Under real conditions, in other words, when all aerodynamic losses are included, the power coefficient cannot be higher than 0.593 [33].

3
Computational Fluid Dynamics(CFD)

Computational fluid dynamics (CFD) is a method of solving the behavior of fluids in a given system and their relationship with each other (heat transfer, reaction, etc.) by computer based systems. The basis of the CFD method was first laid out by Richardson (1910), Courant, Friedrichs, and Lewy (1928) as a result of their studies on the motion of fluids and their computational methods [34]. This method is a powerful tool for understanding fluid behavior in industrial and non-industrial applications. The main fields where computational fluid dynamics are used are below.

- Aerodynamic applications of land and aircraft
- Hydrodynamic applications of floating vehicles
- Turbomachinery
- Cooling applications of electronic circuits
- Combustion efficiency applications in internal combustion engines and gas turbines
- Design and efficiency applications of chemical process equipment and processes
- Determination of indoor and outdoor air quality in buildings
- Amount and diffusion applications of pollutants
- Biomedical applications

The first investment costs of the product can be reduced by the CFD method decreasing the number of experiments and prototypes. The CFD method can depict the fluid system and related physical events in detail. At the same time, the CFD method is an effective and powerful design tool in the absence of prototyping or testing. The advantages of the CFD method are as following.

- Significantly reduce design costs and time
- Necessary experiments could be in a more conscious and controlled manner
- Minimizing security scenario and danger risks
- Quickly revealing desired results

Computational fluid dynamics provides solution to flow problems by using numerical based algorithms. In general, these algorithms have a user interface. The model prepared through this interface is defined to the program and then the solution is made by specifying the boundary conditions. There are codes used for commercial purposes in the market. In general, some of these codes can be listed as ANSYS Fluent, ANSYS CFX, StarCCM, OpenFoam, FloEFD, Comsol.

The steps required for performing a CFD analysis are as below.

- Determination of the purpose of the analysis
- Creation and Preparation Geometry for Calculation
- Generation of Mesh
- Definition of Required Physics and Boundary Conditions
- Solution
- Post-processing

Generally, in an analysis, about 50% of the time is taken by determining the control volume and forming the mesh. Proper and accurate generation of the mesh is very important for the accuracy of the analysis.

3.1 Determination of the Purpose of the Analysis

Computational fluid dynamics offers a wide range of applications to users today. However, this wide area of use can sometimes lead to undesirable situations such as complicating problems and inability to achieve results. Before starting the analysis, users should know exactly which parameter they want to see with which accuracy, where and how fast. It is necessary to make certain assumptions since it will be impossible to directly analyze real life events. Care should be taken that these assumptions and approaches do not contradict the physics of the event.

3.2 Creation and Preparation Geometry for Calculation

After determining the purpose of analysis, the geometry to be analyzed by CFD as the second step should be revealed with CAD software. There are many professional CAD programs on the market such as Solidworks, Catia, NX Siemens. The structural elements on the geometry (bolts, screws, etc.) do not need to be modeled on CAD since the flow and its effects are investigated in computational fluid dynamics analyzes. If the CAD geometry to be analyzed is taken from outside, these parts must be cleaned and the flow volume removed. In general, surfaces with small radius of curvature in the computational domain should be removed as long as they do not have a critical impact on the flow. In this way, the quality of the mesh will be increased and the number of solutions will increase by decreasing the number. If the thermal elements for the solid side are to be considered in the analyzes, solid parts should be included in the analysis when preparing the model.

3.3 Generation of Mesh

The set of equations solved in computational fluid dynamics analysis is called governing equations. These equations are nonlinear partial differential equations. A number of discretization methods are applied in solving these sets of equations. On the basis of discretization methods; The model to be analyzed is divided into 2 or 3 dimensional finite fields / volumes and the equation sets to be solved are made linear. These elements are called mesh. The structure of a mesh is like below.

- Node
- Edge
- Face
- Cell
- Zone

Mesh structure is seen in Figure 3.1.

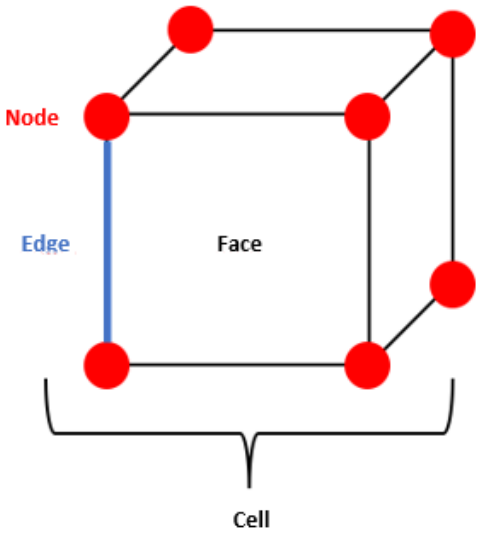

Figure 3.1 The structure of a mesh

Mesh types are generally divided into two groups as structured mesh and unstructured mesh. Structural mesh consist entirely of rectangular elements. On the other hand, unstructured mesh consist of triangular elements. 2 and 3-dimensional representation of these elements are given in Figure 3.2.

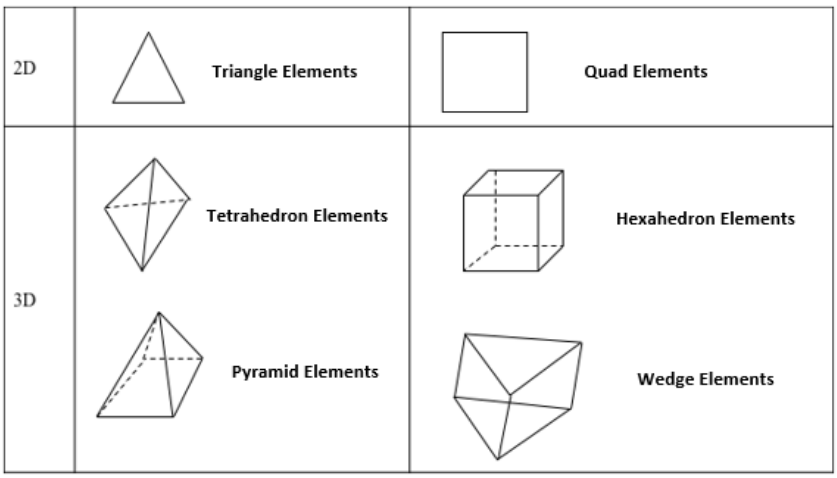

Figure 3.2 Element types of mesh

The amount of mesh should be carefully adjusted. Mesh, which are used more than necessary, bring economic burden and increase the margins of error caused by the increased matrix size.

3.3.1 Governing Equations of the Flow

The conservation equations of fluid flow, whose motion is expressed in terms of velocity, pressure, temperature and their derivative by time and location. The conservation equations for steady incompressible flows in cartesian coordinates are given below.

Continuity Equation

$$\frac{\partial u}{\partial x}+\frac{\partial v}{\partial y}+\frac{\partial w}{\partial z}=0, \tag{3.1}$$

Momentum equations are given below in the x, y and z directions, respectively;

$$u\frac{\partial u}{\partial x}+v\frac{\partial u}{\partial y}+w\frac{\partial u}{\partial z}=-\frac{1}{\rho}\frac{\partial p}{\partial x}+\nu\left[\frac{\partial^2 u}{\partial x^2}+\frac{\partial^2 u}{\partial y^2}+\frac{\partial^2 u}{\partial z^2}\right], \tag{3.2}$$

$$u\frac{\partial v}{\partial x}+v\frac{\partial v}{\partial y}+w\frac{\partial v}{\partial z}=-\frac{1}{\rho}\frac{\partial p}{\partial y}+\nu\left[\frac{\partial^2 v}{\partial x^2}+\frac{\partial^2 v}{\partial y^2}+\frac{\partial^2 v}{\partial z^2}\right], \tag{3.3}$$

$$u\frac{\partial w}{\partial x}+v\frac{\partial w}{\partial y}+w\frac{\partial w}{\partial z}=-\frac{1}{\rho}\frac{\partial p}{\partial z}+\nu\left[\frac{\partial^2 w}{\partial x^2}+\frac{\partial^2 w}{\partial y^2}+\frac{\partial^2 w}{\partial z^2}\right], \tag{3.4}$$

In these equations ρ density (kg/m^3); velocities in the x, y, z direction (m/s), respectively, in u, v, w; p pressure (Pa); υ (m^2/s) represents kinematic viscosity.

3.3.2 Turbulence Modelling

The turbulent flow modeling is based on the time averages of the Navier-Stokes equations Reynolds made in 1895. With this study terms describing turbulence were obtained and named as Reynolds stresses. In order to describe these stresses mathematically, Boussinesq introduced the concept of eddy viscosity. In 1904, he discovered the boundary layer and made progress in turbulence. The "mixing length" approach Boussinesq used to calculate the eddy viscosity was developed by Prandtl. Then, studies on turbulence modeling have been made with reference to this study. Today, models based on the “mixing length” approach are called "zero equation models". Obtaining more realistic mathematical expressions for turbulence stresses is very important in determining the properties of turbulent flow. Eddy viscosity is described in terms of kinetic energy (k) of turbulence oscillations in the model known as the "one equation model" proposed by Prandtl, and taking into account the effect of the flow history. In 1942, in addition to turbulence kinetic energy, Komogorov proposed a new equation for the damping ratio (ω) of energy in unit time and volume.

As a result, in addition to conservation equations, k-ω model included two more equations for obtaining eddy viscosity and modeling of turbulence. Over time, this model was discovered as a "two equation model" equation.

The k-ω model has become more widely used in boundary layer solutions because of the separation of flow, turbulence transition zones solution and low Re number, since it provides more accurate results than the k-ϵ model. For this reason, k-ω model was preferred in the analyzes performed in the studies conducted. Additionaly in study of Krogstad and Adaramola, Three dimensional computational fluid dynamics (CFD) simulations were performed by using k-ω turbulence model [17].

3.3.3 Moving Reference Frame

Flow equations can be written for a rotational stationary frame. In this way, it is possible to take account of the rotational effects for steady-state analysis. First, the rotational parts of the geometry are defined in a static volume. The rotational motion are then specified to this generated volume. Detailed theoretical aspects of the moving reference frame method are given below [34].

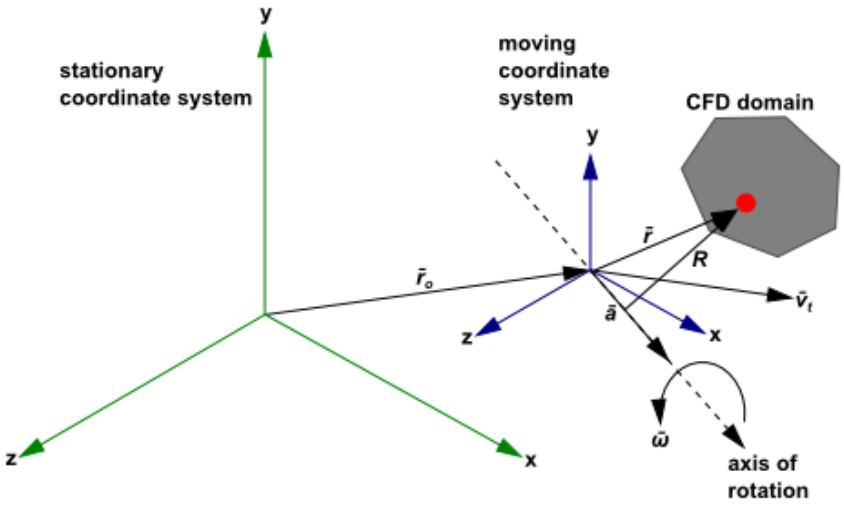

Figure 3.3 Vector transformations between moving and stationary frames [34]

The rotation axis is defined with a unit vector represented by α like below.

$$\boldsymbol{\omega}' = \omega \boldsymbol{\alpha}' \tag{3.5}$$

If position vector r' is created from the stationary coordinate system to the moving coordinate system, it can be converted as the fluid velocity.

$$\boldsymbol{v}_r^{'} = \boldsymbol{v}^{'} - \boldsymbol{u}_r^{'} \tag{3.6}$$

Here $v_r^{'}$ is the relative speed relative to the moving frame and $v^{'}$ is the absolute speed. Fluid velocity can be defined like below in the moving frame.

$$\boldsymbol{u}_r^{'} = \boldsymbol{v}_t^{'} + \boldsymbol{\omega}^{'} \times \boldsymbol{r}^{'} \tag{3.7}$$

Here $v^{'}$ is defined as the transition speed between stationary and moving frames. Normally, $\omega^{'}$ and $v_t^{'}$ are time-dependent variables. The increase in the acceleration in the flow in the rotational frame is expressed by the variables added to the momentum equations. At the same time, momentum equations for moving rotational frames can be written according to absolute velocity and relative velocity. Momentum equations based on relative velocity were used in the analyzes. Mass and momentum equations provided below in terms of relative velocity.

Continuity equation according to relative velocity

$$\frac{\partial \rho \boldsymbol{v}_r^{'}}{\partial t} + \nabla \rho \boldsymbol{v}_r^{'} = 0 \tag{3.8}$$

Momentum equations according to relative velocity

$$\frac{\partial \rho \boldsymbol{v}_r^{'}}{\partial t} + \nabla(\rho \boldsymbol{v}_r^{'} \boldsymbol{v}_r^{'}) + \rho(2\boldsymbol{\omega}^{'} \boldsymbol{v}_r^{'} + \boldsymbol{\omega}^{'} \boldsymbol{\omega}^{'} \boldsymbol{r}^{'} + \boldsymbol{\alpha}^{'} \boldsymbol{r}^{'} + \boldsymbol{a}^{'}) = -\nabla p + \nabla \boldsymbol{\tau}_r^{'} + \boldsymbol{F}^{'} \tag{3.9}$$

In momentum equation $2\omega^{'} v_r^{'}$ represents coriolis acceleration and $\omega^{'} \omega^{'} r^{'}$ represents centripetal acceleration. The terms associated with α refer to time-dependent change. Since the rotation speed is constant in the analyzes, the terms related to α can be omitted.

$$\alpha = \frac{\partial \boldsymbol{v}_r^{'}}{\partial t} \Rightarrow \frac{\partial \boldsymbol{\omega}^{'}}{\partial t} \tag{3.10}$$

3.4 Definition of Required Physics and Boundary Conditions

A well-defined physical properties and boundary conditions are required, as well as a high quality mesh, to achieve the correct solution in computational fluid dynamics analysis. False boundary conditions cause false results. When defining the problem, it is necessary to select the correct models and to create a suitable mesh. At the same time, the properties of the materials used must be selected in accordance with the conditions to be simulated. For example, let us assume that an air movement at 50 °C should be modeled if the program defines the density of air at 25 °C, although there is no problem in the convergence of analysis, the results will likely not reflect the reality.

3.5 Solution

Prepared CFD models are solved in computer environment. The selection of the methods used to make the solutions is effective in the convergence of the analysis. The use of incorrect numerical methods may lead to divergence of the analysis despite the correct boundary conditions. The desired values should be visualized and the change should be monitored while solving the analyzes. In this way, the analysis is completed according to the convergence situation.

3.6 Post-processing

After the solution is completed, the results can be visually examined to see the behavior of the flow. Velocity fields and vectors, streamlines, pressure fields are visualized to reveal problematic areas. After revealing these regions, necessary improvements are made in the CAD model and the analyzes are repeated to minimize the problematic regions.

4
Methods

ANSYS Fluent R2019 R1 has been used for the present case. Second order upwind scheme was used for discretization and coupled algorithm was used for velocity-pressure coupling. In order to resolve viscous sublayer, RANS - SST k-ω turbulence model has been used. Whole analyses have been performed as steady state pressure based, and proper mesh resolution has been used for near wall and volume mesh. Therefore, y^+ is important to resolve the viscous sublayer for the validation and diffuser optimization, and y^+ is kept under 5 to ensure that the viscous sublayer is properly resolved.

4.1 Validation

At the beginning of the study, validation has been performed for wind turbine of which experimental performance characteristics are provided in detail by Krogstad and Adaramola [6] with study performed in the wind tunnel of Department of Energy and Process Engineering at The Norwegian University of Science and Technology. A large set of experimental datum is published, and for the validation has been carried out with comparison of the power coefficient and thrust coefficient.

The flow volume is generated from 3D CAD geometry using the SpaceClaim Direct Models (SCDM) program. Turbine should not be affected from other boundary conditions with a rotor diameter of 0.9 m. Flow volume created as eight times bigger than diameter of turbine, and turbine is 6m far from inlet also 16m far from outlet. The geometry used in the analysis is given in Figure 4.1.

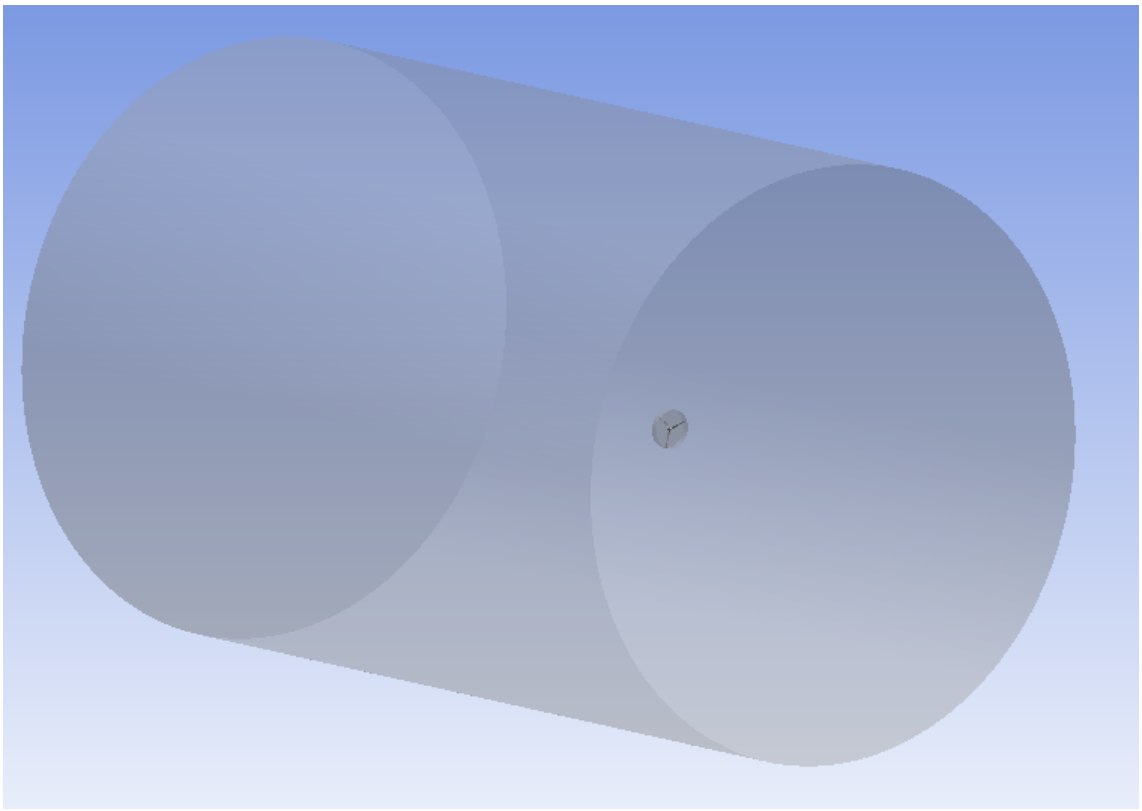

Figure 4.1 Flow volume of validation geometry

Moving reference frame (MRF) method is used in the modeling of rotational parts in computational fluid dynamics analyses. Therefore, the geometry created is prepared in accordance with the MRF method. The image of MRF geometry details are given in Figure 4.2.

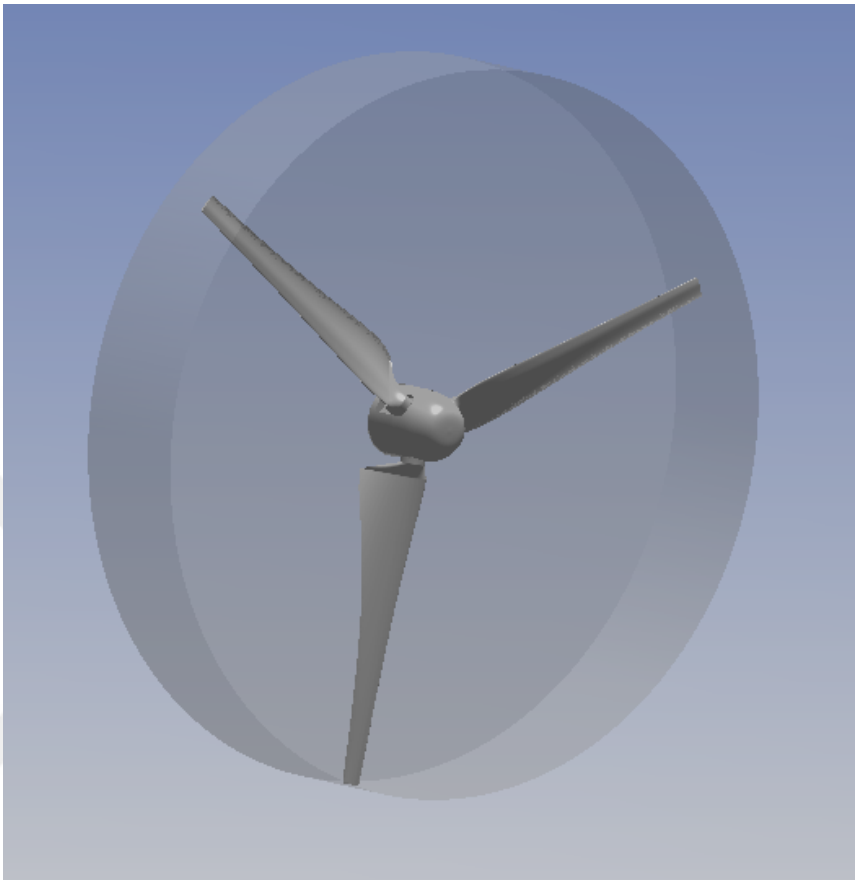

Figure 4.2 The Image of MRF geometry

The mesh is generated with tetrahedral elements in ANSYS Meshing, and the mesh volume converted to polyhedral mesh in ANSYS Fluent. The image of the mesh is shown in Figure 4.3 and Figure 4.4 .

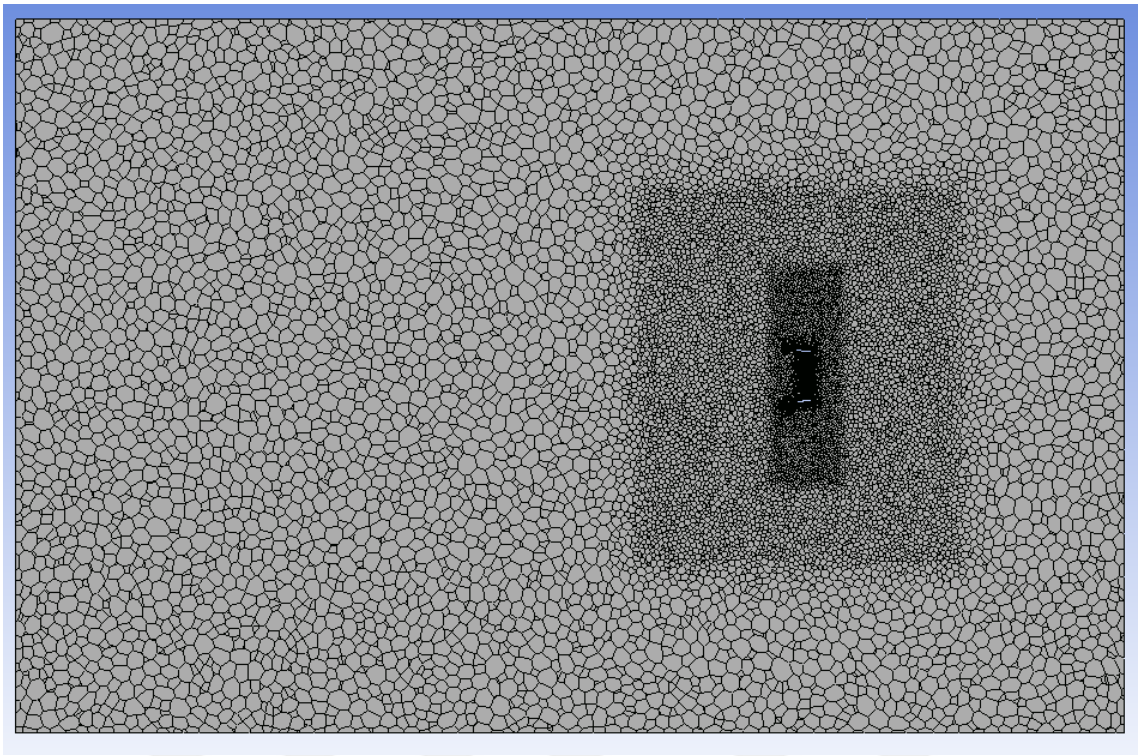

Figure 4.3 The image of the mesh-1 ($y^+ \approx 1$)

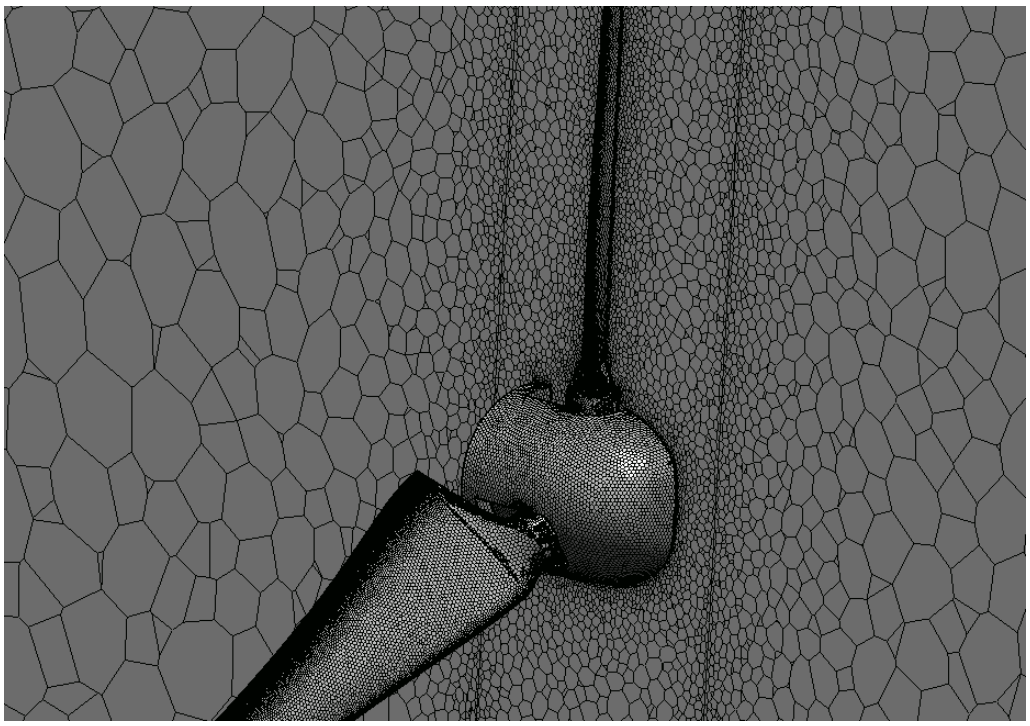

Figure 4.4 The image of the mesh-2 ($y^+ \approx 1$)

Some assumptions are made in the analysis. These assumptions:

- The flow regime is turbulent and the solution is steady state.
- In the analysis, energy equations are not solved because there is no heat transfer in the flow.

Rotating effect of the turbine is solved by moving reference frame (MRF) method.

Firstly, mesh independence tests are carried out for 6 different meshes at 9 m/s free wind speed for open rotor wind turbine as shown in Figure 4.5 and Table 4.1. Proper number of mesh was 2.8 million elements.

Table 4.1 Mesh independence cases information for Open Rotor Turbine

Case	Mesh Number (10^6)	Tork(Nm)
1	0,8	0,9825
2	0,9	1,0332
3	1,4	1,0544
4	2,1	1,0049
5	2,8	0,9866
6	4,6	0,9834

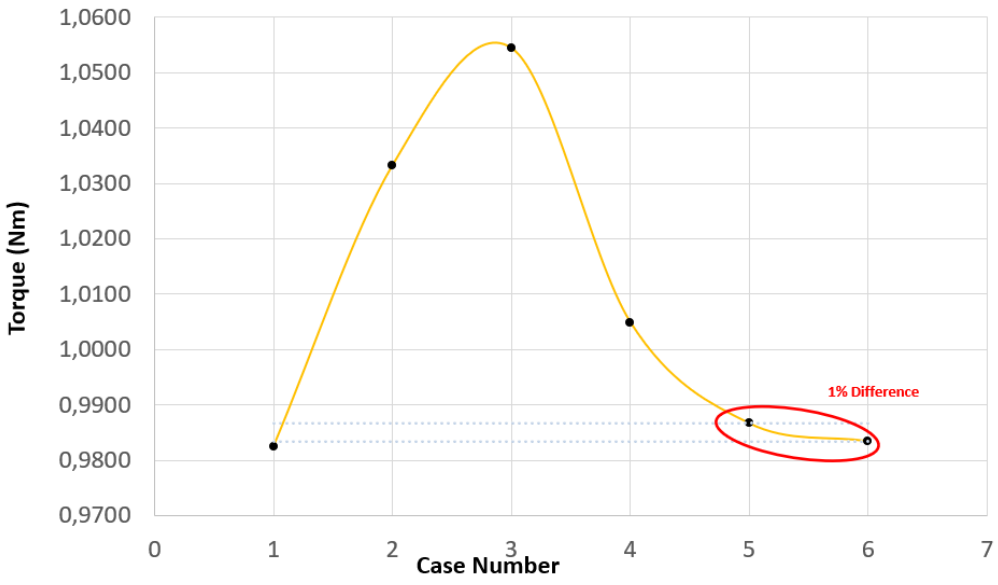

Figure 4.5 Mesh independence study in CFD for Open Rotor Turbine

For the validation, CFD results are compared with experimental data. The CFD results exhibit very close values to experimental data. Power coefficient and thrust coefficient can be found for the variable tip speed ratio (TSR) in the Figure 4.6 and Figure 4.7.

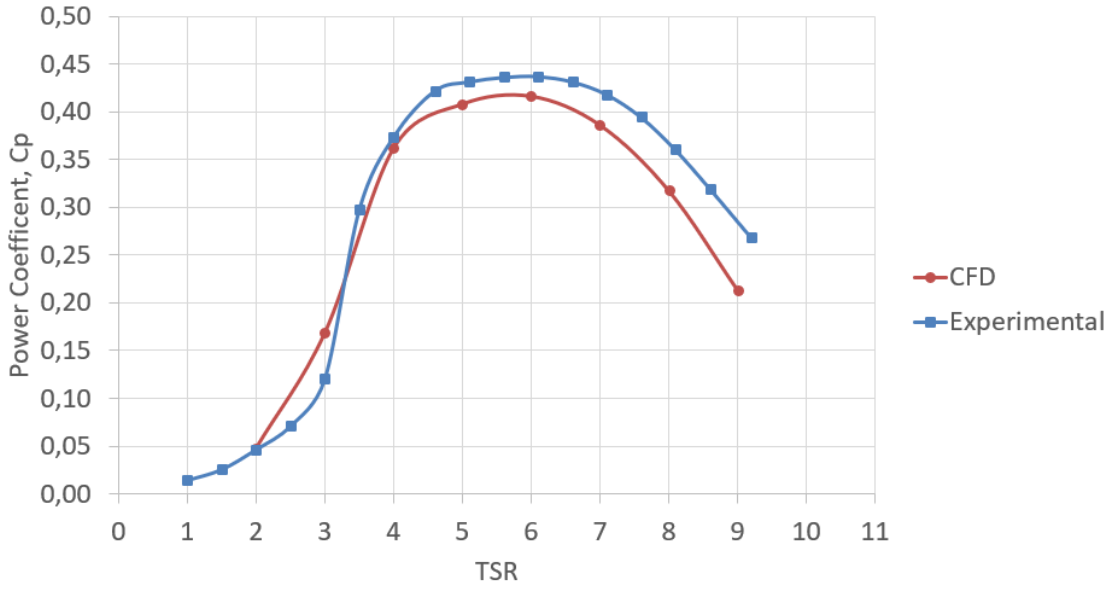

Figure 4.6 Comparisons of power coefficients from CFD with the measurements

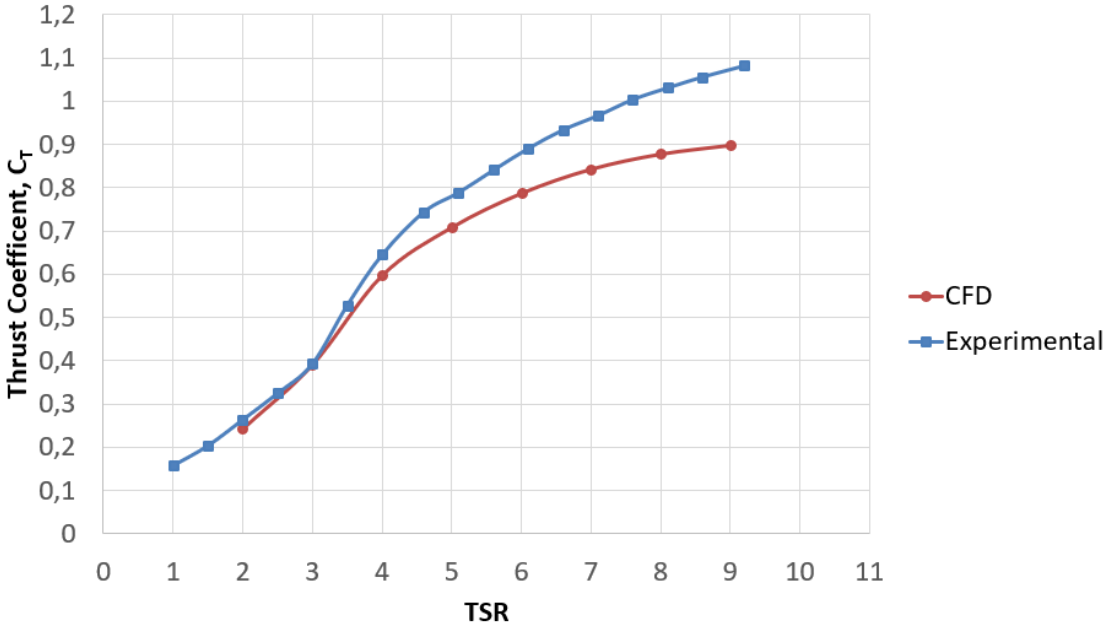

Figure 4.7 Comparisons of thrust coefficients from CFD with the measurements

4.2 Optimization

For this validated wind turbine, a diffuser based on an asymmetrical GOE431 airfoil has been optimized with response surface optimization method in "Ansys DesignXplorer".

It is required to arrange parameters for the components to be improved in design, while using the DesignXplorer method. In the first stage, the program creates a certain number of analysis scenarios using experimental design methods with different parameter groups. The analysis of these scenarios and the relationships between the parameters are determined. The best design point is obtained for the desired situation by using these relationships. The improvement steps are as follows.

- Creating the initial design
- Setting parameters for the regions to be improved
- Creating automatic scenarios from parameters created with the DesignXplorer module
- Analyzing scenarios
- Forming the response surface according to the analysis results
- According to the design objective, creating the new values with response surface.
- Updating the design for optmized design

Uniform wind velocity of 9 m/s is set at the inlet boundary of the computational domain which is the same as one that in experimental study of the tested turbine. Also, the computational model is prepared as 2D axisymmetric swirl in order to represent rotating diffuser in CFD. Diffuser is 8m far from inlet also 11m far from outlet. It is shown in the Figure 4.8 and Figure 4.9.

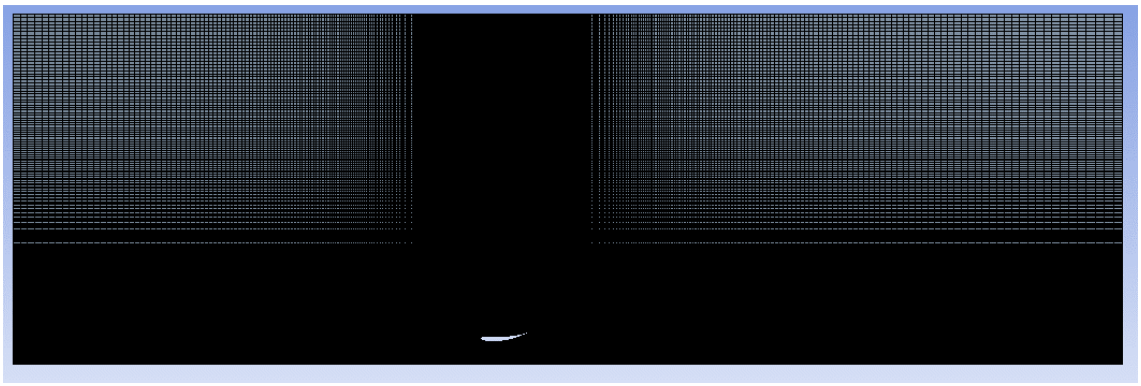

Figure 4.8 2D Axisymmetric swirl model and mesh

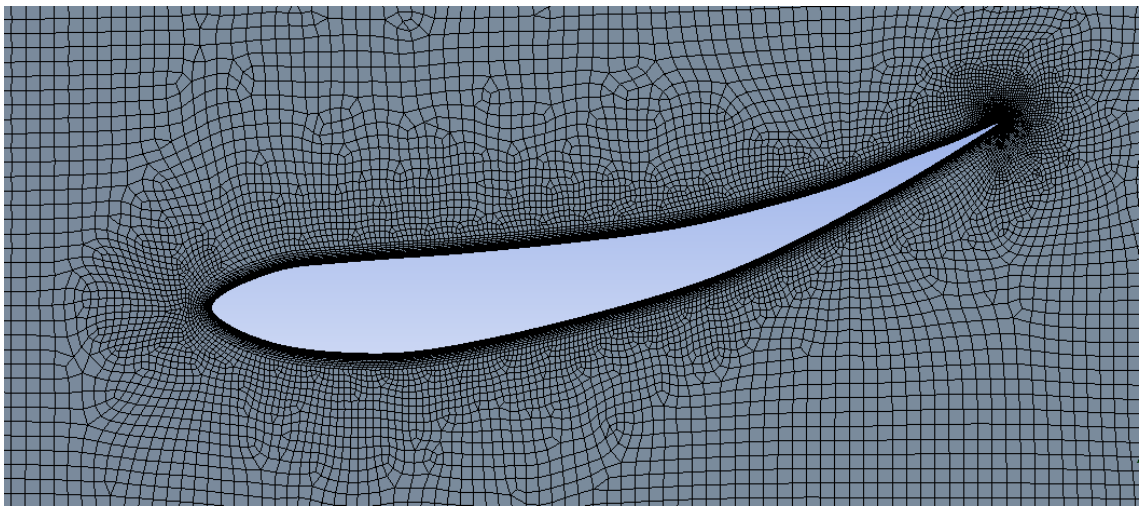

Figure 4.9 Near wall mesh resolution ($y^+ \approx 1$)

For several mesh configurations, the mass flow rate of the diffuser was analyzed, and a mesh independence assessment was performed. The mesh independence results can be seen in Figure 4.10 and Table 4.2 showing minimized differences. Proper number of mesh elements is 266 thousand.

Table 4.2 Mesh independence cases information for diffuser optimization

Case	Mesh Number (10^4)	Mass Flow (kg/s)
1	0.4	9,78
2	1.2	11,12
3	1,9	12,52
4	3,5	12,1
5	4,5	12,74
6	5,6	13,43
7	6,9	13,07
8	8,3	12,93
9	11,5	13,18
10	13,2	13,59
11	26,6	13,75
12	59,1	13,86

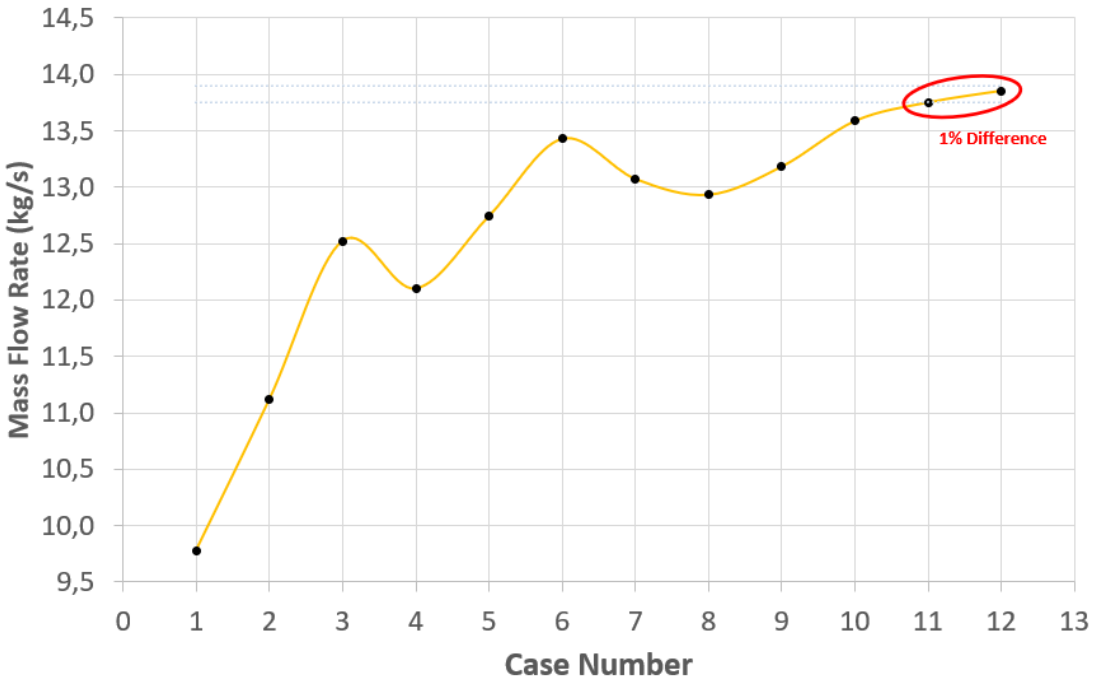

Figure 4.10 Mesh independence for diffuser optimization

4.2.1 Preparation of Parametric Geometry

Parametric geometry is generated with "ANSYS SCDM Scripting". Python Script can be found in the appendix A. Two different parameters have been selected to be optimized. These parameters are the chord length and angle of attack(α) of the diffuser airfoil. Chord length range is from 0.2 m to 0.7 m, and angle of attack range is from 2° to 20°. The goal is to maximize the mass flow rate while maintaining velocity distribution as uniform as possible at the rotor plane by uniformity index of velocity.

The uniformity index represents how a given field variable changes on a surface, where a value of 1 indicates the highest uniformity. The uniformity index is weightable by area or mass: the area-weighted uniformity index captures the quantity change. The mass-weighted uniformity index captures the variation of the flux. The area-weighted uniformity index (γ_a) of a specified field variable ϕ is calculated using the following equation:[34]

$$\gamma_a = 1 - \frac{\sum_{i=1}^{n}[(\left|\phi_i - \phi_i^{'}\right|)A_i]}{2\left|\phi_a^{'}\right|\sum_{i=1}^{n}A_i} \tag{4.1}$$

Where i is the facet index of a surface with n facets, and $\phi_a^{'}$ is the average value of the field variable over the surface:[34]

$$\phi_a^{'} = \frac{\sum_{i=1}^{n}\phi_i A_i}{\sum_{i=1}^{n}A_i} \tag{4.2}$$

Parameters are calculated for the exit plane of the diffuser. The summary of parameters can be seen in Table 4.3.

Table 4.3 Optimization conditions and objectives

Parameter	Type	Lower Bound	Upper Bound	Objective
Chord Length (m)	Input	0,2	0,7	-
Angle of Attack (°)	Input	2	20	-
Mass Flow Rate (kg/s)	Output	-	-	Maximum
Uniformity of Velocity	Output	-	-	Maximum

4.2.2 Response Surface Optimization

Understanding the interrelation of inputs and outputs between each other plays an important role in engineering designs. With the number of parameters increasing

the number of experiments increase to understanding these relationships. This is often costly and time consuming. Therefore, in modern engineering calculations, it is essential to reveal the whole relationships by making experimental designs with inputs and outputs in a shorter time. Central Composite Design was chosen as the experimental design method used in the analysis. Kriging algorithm was used for surrogate model.

4.2.2.1 Central Composite Design

The central composite design (CCD) method is a level 5 differential factorial response surface model. 3 types of composite design models are available. These are circumscribed, inscribed, and face centered central composite design models. There are lower and upper limits in the design space for each factors. Each design factor is represented in a 5-level factor space [-a,-1,0,+1,+a]. The range [-1, + 1] subserves to the physical upper and lower limits of the discovered factor space. The range [-a,+a] indicates the physical lower and upper limits for whole factors. The value "a" is a variable factor depending on the design and the number of factors. In the restricted composite design method, the a value is greater than 1. The inscribed composite design method is represented by figure 4.11 [34].

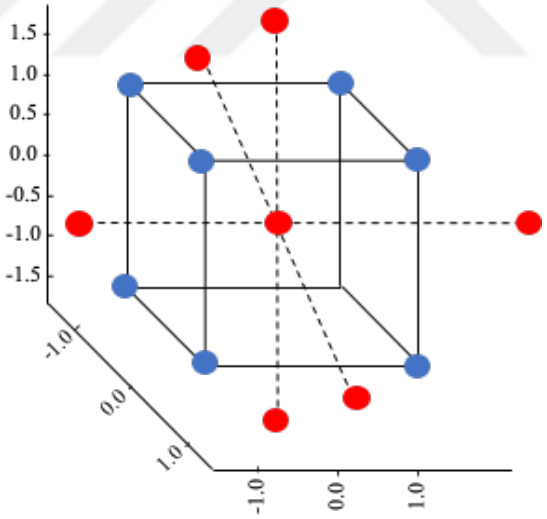

Figure 4.11 Inscribed composite design method factor space

The physical lower and upper limits in the circumscribed composite design space are limited to [-1,+1]. The 5-level factor space in the circumscribed composite design is [-1,-1/a,0,+1/a,+1]. The circumscribed composite design method is represented by Figure 4.12 [34].

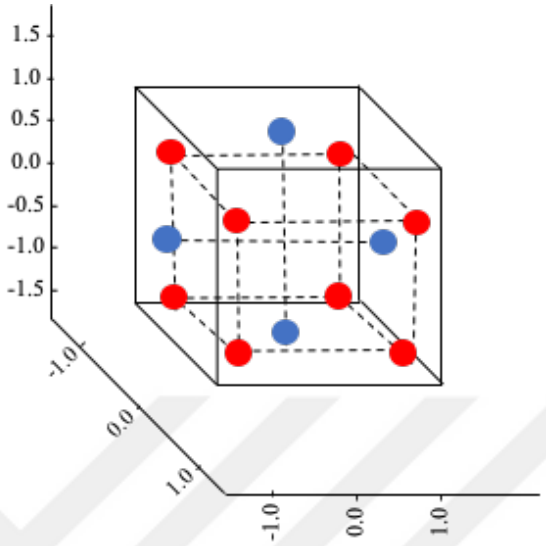

Figure 4.12 Circumscribed composite design method factor space

In the face-centered composite design method "a" value is 1. Therefore, the face centered design method is matched to 3 levels and each face center is matched to any 2 factors. The face centered composite design method is represented by figure 4.13 [34].

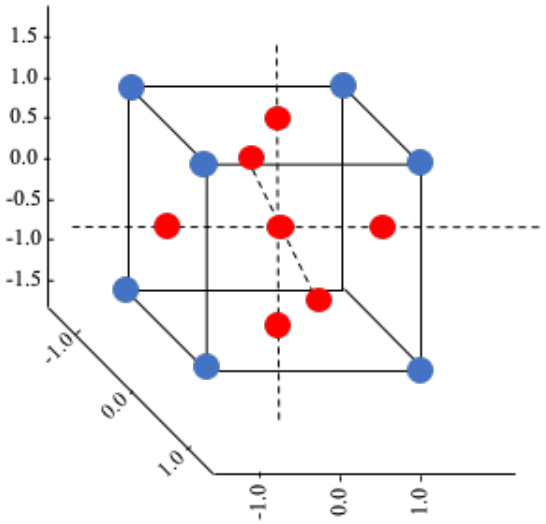

Figure 4.13 Face centered composite design method factor space

4.2.2.2 Kriging

The Kriging method was used as a surrogate because it improved response quality and placed higher order variations of the output parameter. In Kriging, the one-dimensional response value from a simulation is estimated by a generally known polynomial and random separation from the polynomial:[34]

$$y(x) = f(x) + Z(x) \tag{4.3}$$

where y(x) is the unknown answer, f(x) is a polynomial function of x, and Z(x) is considered to be a Gaussian random operation with zero mean, σ^2 variance, and a non-zero covariance. The f(x) term is similar to the polynomial model on a response surface and provides a "global" model of the design space. When approaching the "globally" design space, Z(x) creates "localized" deviations so that the Kriging model interpolates the sample data points. The covariance matrix of is given by:[34]

$$Cov[Z(x^i), Z(x^j)] = \sigma^2 R([r(x^i x^j)]) \tag{4.4}$$

where R is the correlation matrix and r(x^i, x^j) is the spatial correlation of the function between any two of the N sample points $x^i and x^j$. R is an N*N symmetric, positive definite matrix with ones along the diagonal. The correlation function r(x^i, x^j) is a Gaussian correlation function:[34]

$$r(x^i, x^j) = exp\left(-\sum_{k=1}^{M} \theta_k \left|x_k^i - x_k^j\right|^2\right) \tag{4.5}$$

The θ_k in eq. (4.5) are the unknown parameters used to fit the model, M is the number of design points, and $x_k^i and x_k^j$ are the kth components of sample points $x^i and x^j$:[34]

Z(x) can be written.

$$Z(x) = \sum_{i=1}^{N} \lambda_i r(x^i, x) \tag{4.6}$$

Response surface method - prepared with high sensitivity - is based on kriging algorithm, and prediction of response surface has highly accurate results. The response surfaces can be found in Figure 4.14 and Figure 4.15.

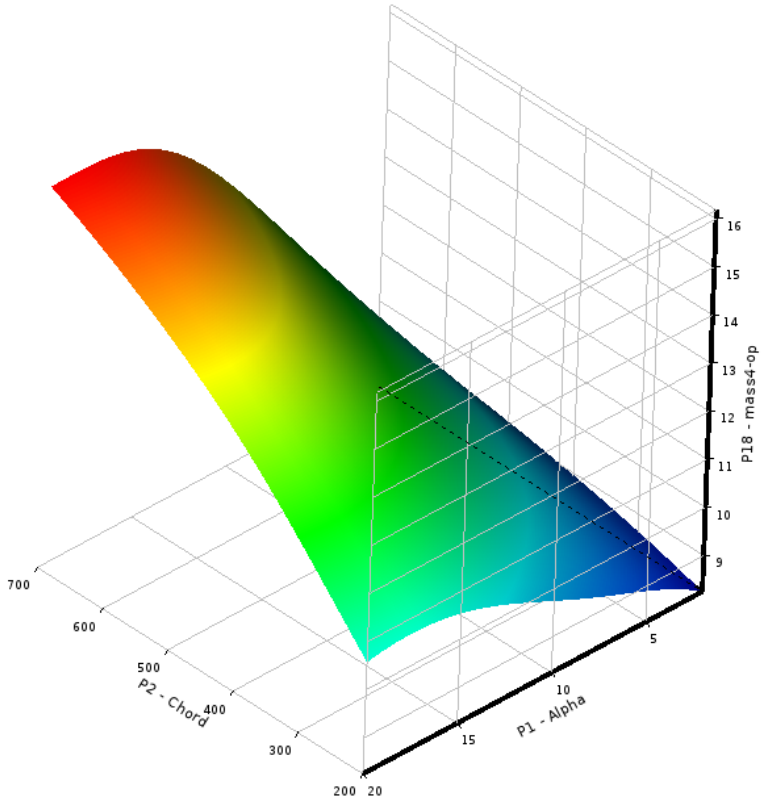

Figure 4.14 Response surface of mass flow rate

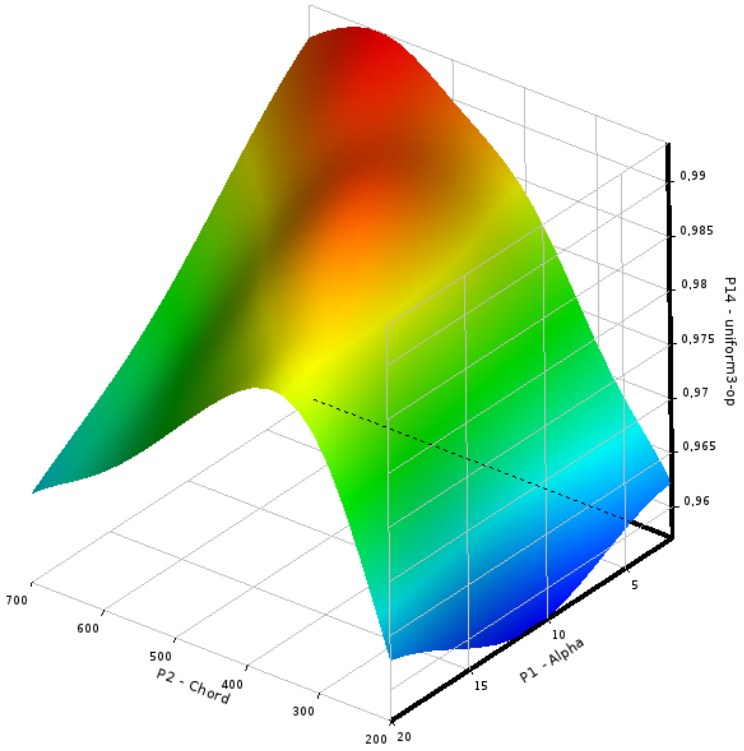

Figure 4.15 Response surface of uniformity of velocity

As a result of the optimization procedure, optimal design candidate is 0.472 m chord length and 13.1 ° angle of attack as shown in Table 4.4 below.

Table 4.4 Optimization results of parameters

Parameter	Type	Lower Bound
Chord Length (mm)	Input	472
Angle of Attack (°)	Input	13,1
Mass Flow Rate (kg/s)	Output	13,47
Uniformity of Velocity	Output	0,988

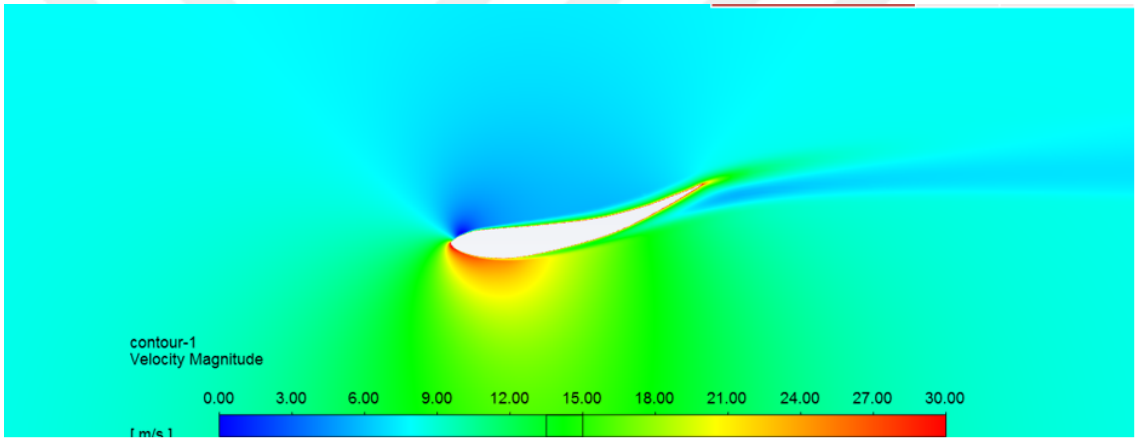

Figure 4.16 Optimal geometry and velocity contour

4.3 Rotor with diffuser

The same mesh structure was used for the other two cases, 2.8 million elements for the open rotor and 7.6 million for the rotor with diffuser cases.

5
Results of Optimized Diffuser for Horizontal Axis Wind Turbine

In this chapter, CFD analysis are performed for the optimal design candidate revealed by response surface optimization. Optimal design candidate examined both as rotating and stationary diffuser.

5.1 Rotating Diffuser

The rotor with rotating diffuser is not suitable for application. Numerical analysis results showed us that the turbine needs a huge torque to rotate. There is excessive friction between the air and the diffuser which prevents the turbine from rotating as illustrated in Figure 5.1.

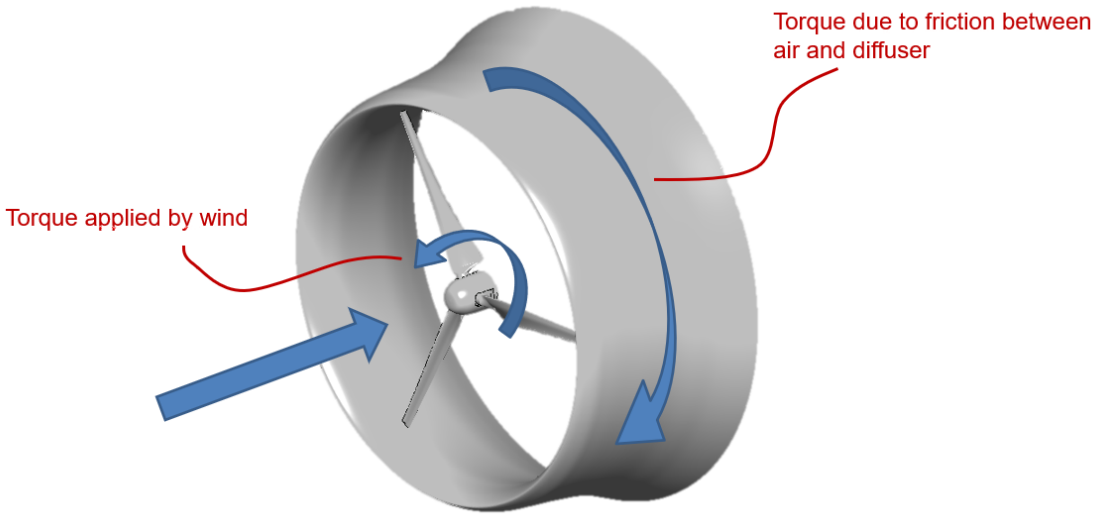

Figure 5.1 Rotating Diffuser

5.2 Stationary Diffuser

The study continued with stationary diffuser, and tip clearance is adjusted as 5 mm. The open rotor wind turbine is compared with rotor with stationary diffuser. Power coefficient (C_p) and thrust (C_T) coefficients versus TSR are depicted in Figure 5.2 and Figure 5.3. These graphics show that the same TSR does not have similar trend between the open rotor and rotor with diffuser. In proper operation of the rotor with diffuser, maximum C_p is expected to be in the higher range of TSR. Blade twist angle must be optimized to achieve higher efficiency in a wider range of TSR.

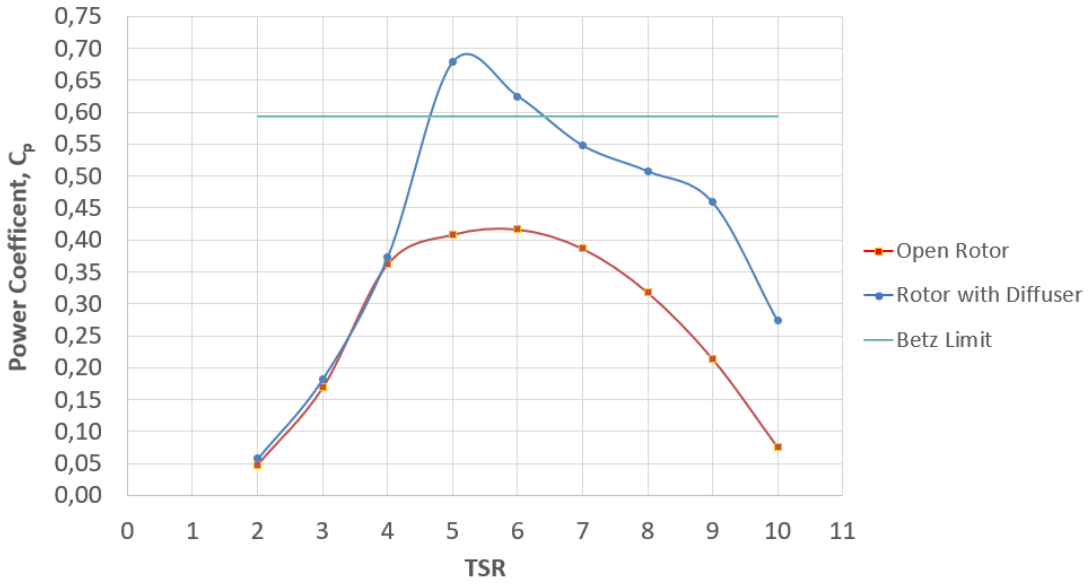

Figure 5.2 Comparisons of power coefficients of "Open Rotor" and "Rotor with Diffuser"

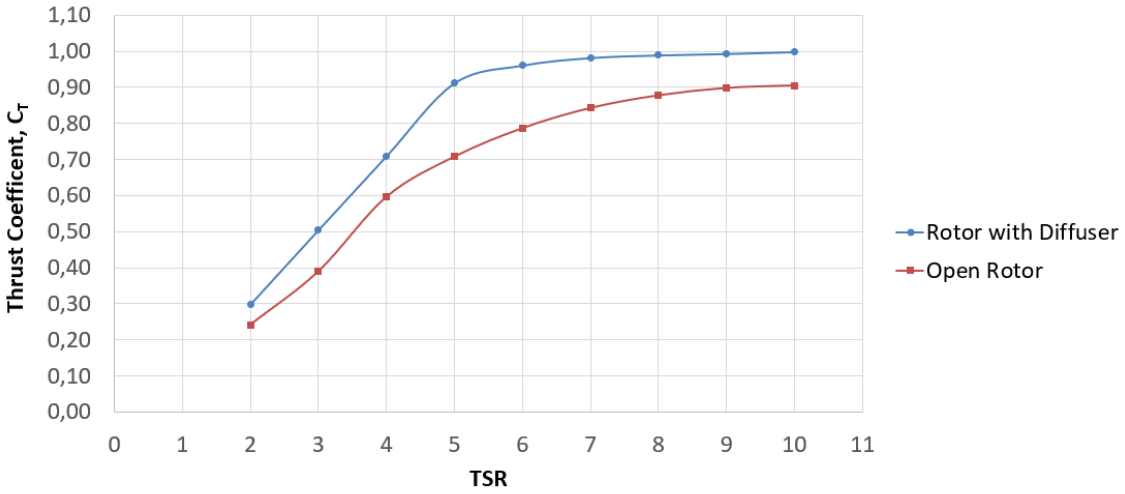

Figure 5.3 Comparisons of thrust coefficients of "Open Rotor" and "Rotor with Diffuser"

Also, the comparison of mass flow rates of blank, only diffuser, open rotor and rotor with diffuser are shown in the Table 5.1 below with same TSR equal to 6.

Table 5.1 Optimization conditions and objectives

Parameter	Mass Flow Rate (kg/s)
Blank	7,014
Diffuser	10,788
Open Rotor	5,652
Rotor with diffuser	6,015

Comparisons of velocities of "Open Rotor" and "Rotor with Diffuser" in longitudinal plane are shown in the Figure 5.4 below.

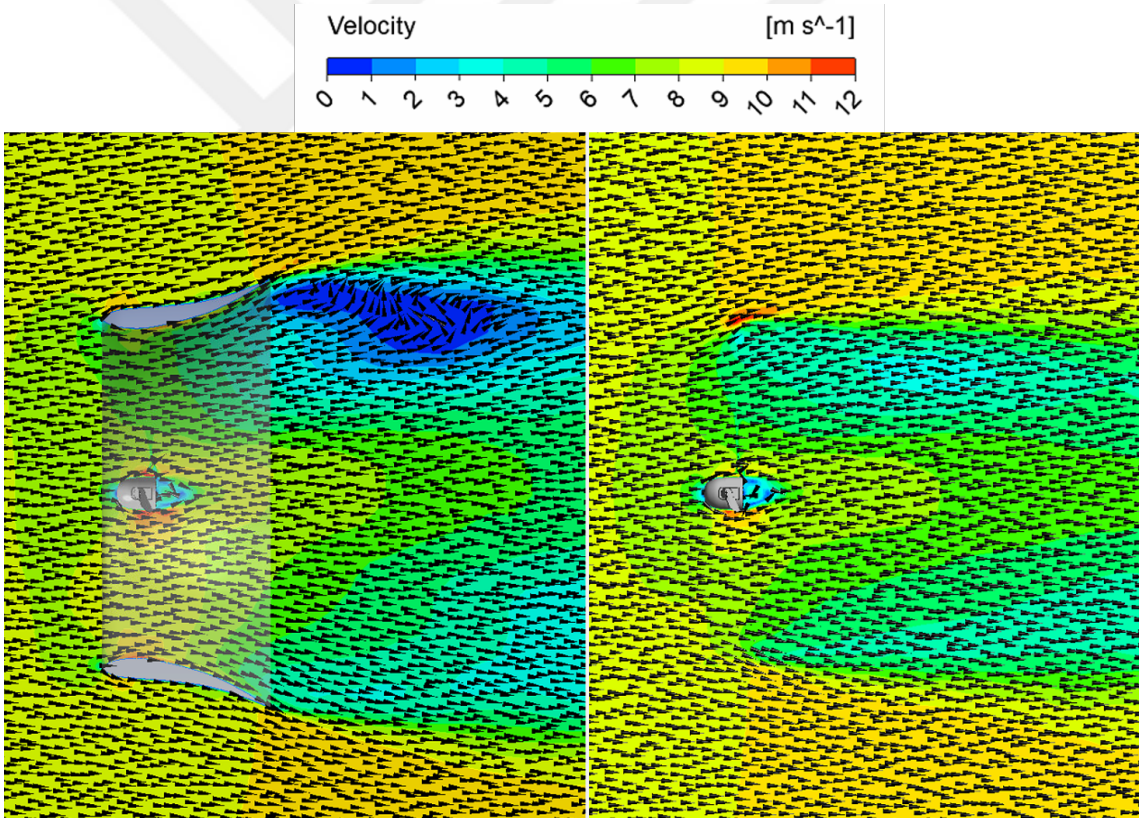

Figure 5.4 Comparisons of velocities of "Open Rotor" and "Rotor with Diffuser" in longitudinal plane

The CFD analysis revealed that a diffuser augmented turbine could accelerate the wind velocity at the wake region and intake of the diffuser, and that is shown in the Figure 5.5 below.

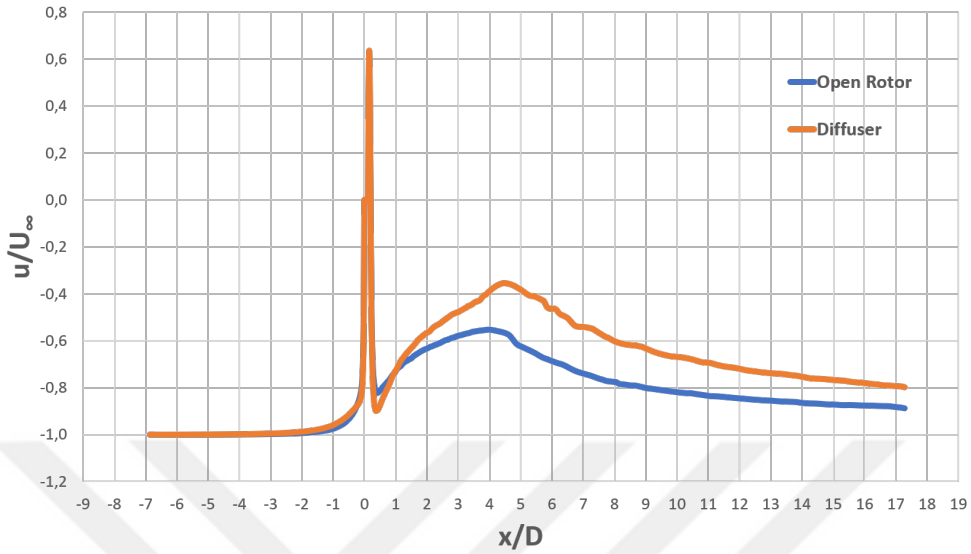

Figure 5.5 Comparisons of streamwise wind velocity distribution on the rotation axis of wind turbine at TSR=6

The diffuser increases the mass flow rate, especially because it increases the velocity on the tip of the blades. This shows that there is no difference in the axial speed before the rotor. The streamwise velocity change in the radial direction before and after the rotor shows the effect of the increase in the mass flow rate of the diffuser for open rotor and rotor with diffuser, and comparisons of sections are shown in the Figure 5.6 and Figure 5.7 below.

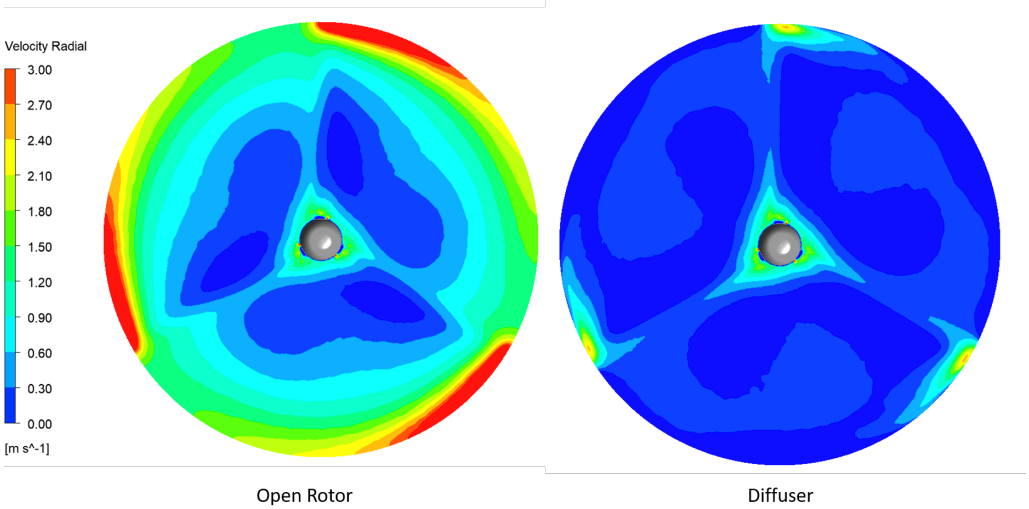

Figure 5.6 Comparisons of radial wind velocity distribution on front section of wind turbine at TSR=6

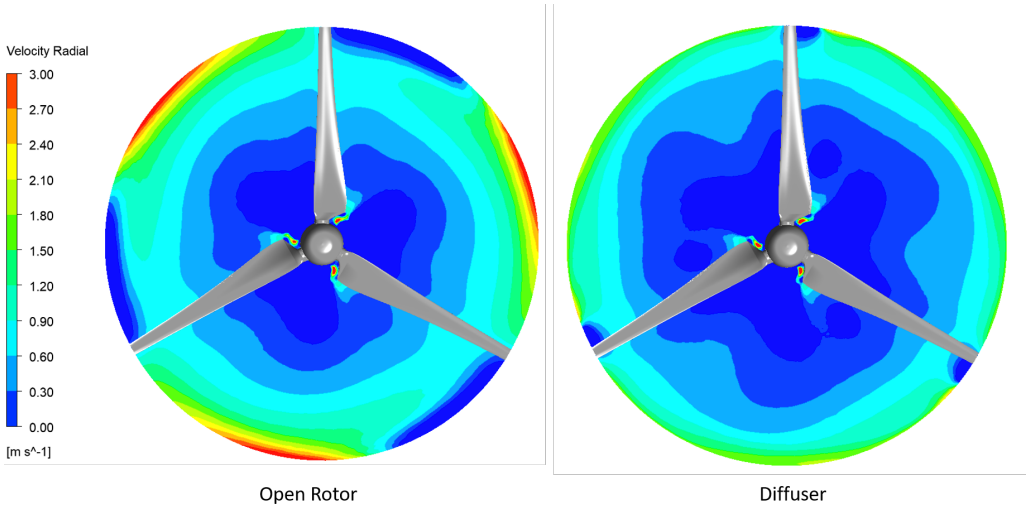

Figure 5.7 Comparisons of radial wind velocity distribution on rear section of wind turbine at TSR=6

To investigate lift due to pressure load, computations are performed, and the pressure coefficients around the blade at some specific radial locations (Equation 5.1) are compared. For comparison four different sections have been investigated. Each section has been created dimensionless radial location based on rotor radius. Diameter of the rotor illustrations can be found in Figure 5.8 below.

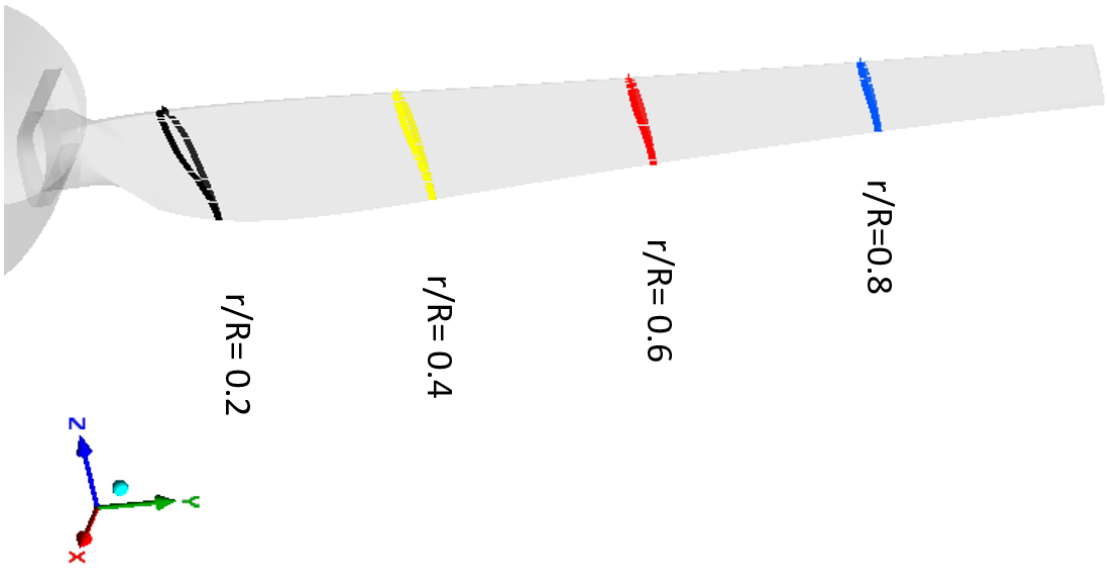

Figure 5.8 Sections of blade

$$C_p^{'} = \frac{(P - P_0)}{\frac{1}{2}\rho U_0^2}, \tag{5.1}$$

A diffuser augmented turbine has a higher wind velocity than an open rotor turbine. That provides higher mass flow. Due to higher wind speed around the turbine blades, negative pressures on the rearward surfaces of the blade increased. This yields to an increase in lift force and in turn results in increase in rotor torque. It is revealed in the Figure 5.9, Figure 5.10 Figure 5.11 and Figure 5.12 below.

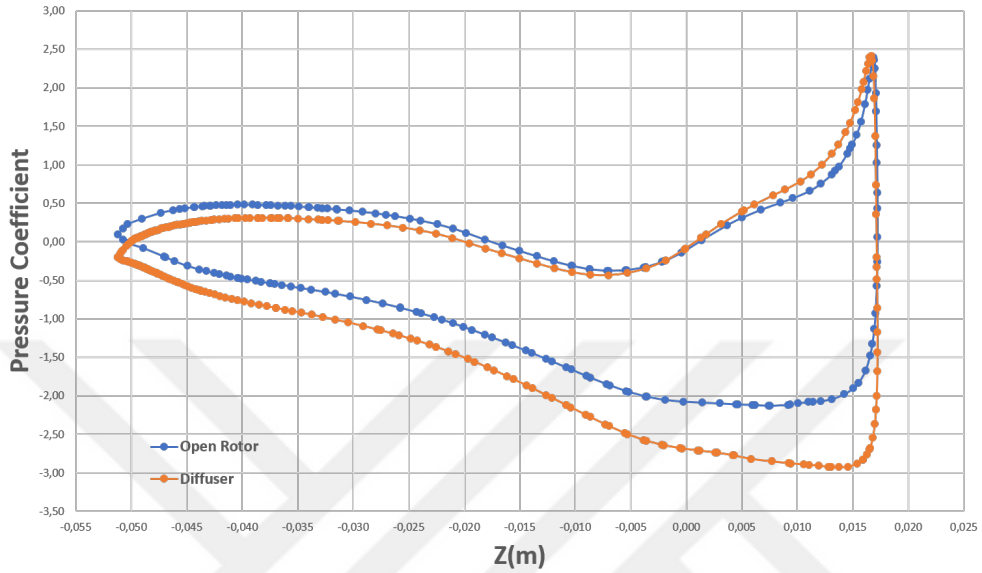

Figure 5.9 Pressure coefficient distributions along section of blade at r/R=0.2 and TSR=6

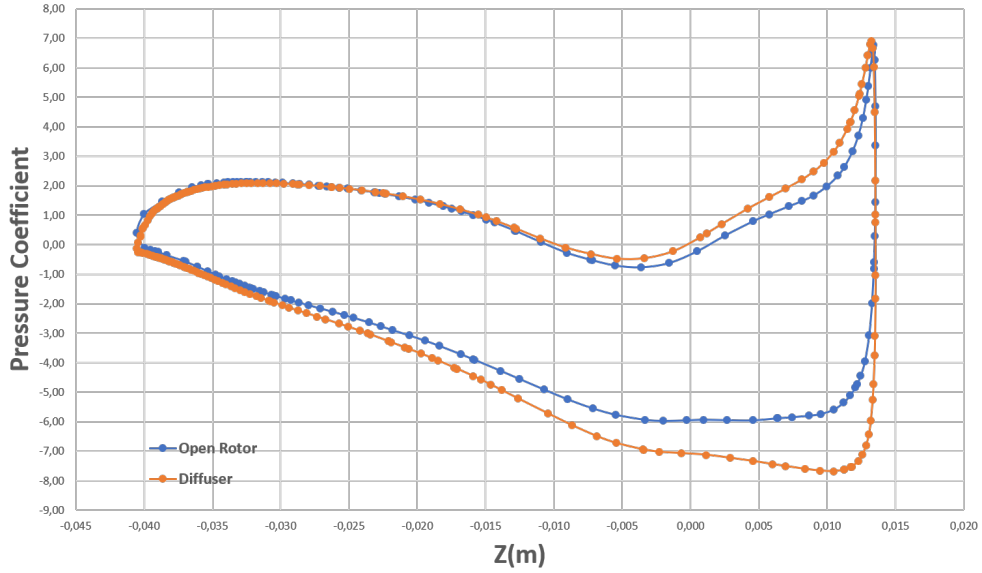

Figure 5.10 Pressure coefficient distributions along section of blade at r/R=0.4 and TSR=6

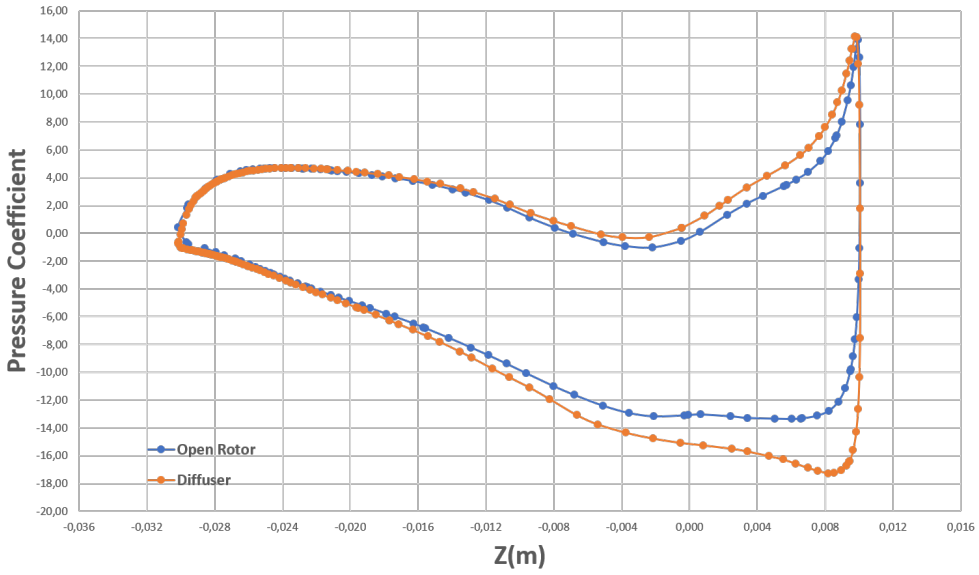

Figure 5.11 Pressure coefficient distributions along section of blade at r/R=0.6 and TSR=6

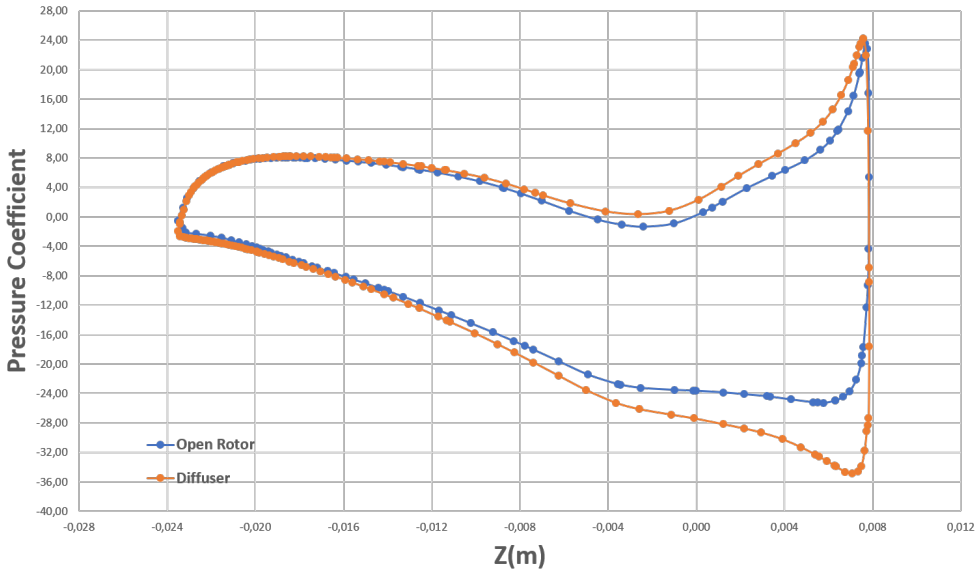

Figure 5.12 Pressure coefficient distributions along section of blade at r/R=0.8 and TSR=6

When the pressure coefficient graph is considered, it shows that the pressure coefficient across a section is effectively higher on the rearward of the blade. This increase indicates more efficient rotation of the rotor. When the chart is examined, the larger area in the negative region of the pressure coefficient of the graph, indicates that the system is more efficient.

6
Conclusions

In this study, first, a wind turbine of which geometry and performance charts are well-documented is validated by CFD. A road map has been developed for simulating wind turbines with diffuser and optimizing a diffuser for wind turbines. Characteristics of a wind turbine with diffuser are investigated by an engineering approach. Then the CFD approach is applied for wind turbine geometries, and the comparison of the power and thrust coefficients results are made with the available experimental results. This will be a guideline for the proper design of wind turbine with diffuser.The numerical methods showed good agreement with the experimental data. Experimental validation is important for CFD analysis. Validation of a main model can be a reference for the resulting simulations.

Developments of diffuser designs is possible via CFD. Chord length and angle of attack can be investigated for diffuser optimization, and optimization methods can be applied to reach higher mass flow rate and uniformity of flow. This optimization methods are able to develop the most effective design point to evaluate an efficient wind turbine. After all, better flow performance and more efficient wind turbine can be useful to be carried out with diffuser.

It can be concluded that rotating diffuser is not effective as stationary diffuser due to its huge friction surface with air. The diffuser should have large size of chord length to increase mass flow rate. However, this makes the diffuser more useless and heavier. Therefore, the engineering approach will continue to be applied to use stationary diffuser in order to increase the power generated from the wind. The power and thrust coefficients were calculated for stationary diffuser in CFD analysis, and eventually betz limit can be exceeded.

For future works, shape optimization will be applied on the rotor blade. Even, different airfoil shape will be tested for the optimization process. Also, tip clearance of the turbine and diffuser will be worked on. Rotor blade twist angle will be considered to increase the efficiency.

A
Ansys SpaceClaim Direct Modeller Python Script

```
# Python Script, API Version = V17

ClearAll()

A = Parameters.Alpha
C = Parameters.Chord

# Set Sketch Plane
sectionPlane = Plane.PlaneXY
result = ViewHelper.SetSketchPlane(sectionPlane, None)
# EndBlock


# Coordinates of section and full version of script can be found with link below.
# https://drive.google.com/open?id=1IuBtu3fXVH75Bv30fat7QCT4EDOrWa7P


# Insert From File
importOptions = ImportOptions.Create()
DocumentInsert.Execute(r"E:\safak\new\GOE431.txt", importOptions, GetMaps("b2cc6649"))
# EndBlock


# Solidify Sketch
mode = InteractionMode.Solid
result = ViewHelper.SetViewMode(mode, None)
# EndBlock

# Fill
selection = Selection.Create(GetRootPart().Curves[0])
secondarySelection = Selection()
options = FillOptions()
```

```
result = Fill.Execute(selection, secondarySelection, options,
    FillMode.ThreeD, None)
# EndBlock


# Delete Objects
selection = Selection.Create(CurveFolder1)
result = Delete.Execute(selection)
# EndBlock


# Rotate About Z Handle
selection = Selection.Create(Body1)
anchor = Selection.Create(CoordinateSystem1)
axis = Move.GetAxis(anchor)
options = MoveOptions()
result = Move.Rotate(selection, axis, DEG(-A), options, Info2)
# EndBlock

# Scale 1 Objects
selection = Selection.Create(Body1)
preserveHoles = False
result = Scale.Execute(selection, Frame.Create(Point.Create(MM
    (0), MM(0), MM(0)),
     Direction.DirX,
     Direction.DirY), Vector.Create(MM(C), MM(C), MM(C)),
    preserveHoles)
# EndBlock


# Translate Along Y Handle
selection = Selection.Create(Body1)
anchor = Selection.Create(CoordinateSystem1)
direction = Move.GetDirection(anchor, HandleAxis.Y)
options = MoveOptions()
result = Move.Translate(selection, direction, MM(-450), options
    , Info1)
# EndBlock



# Create Datum Plane
selection = Selection.Create(Axis1)
result = DatumPlaneCreator.Create(selection, True, Info3)
# EndBlock


```

```
76
77 # Mirror
78 selection = Selection.Create(GetRootPart().Bodies[0])
79 mirrorPlane = Selection.Create(GetRootPart().DatumPlanes[0])
80 options = MirrorOptions()
81 result = Mirror.Execute(selection, mirrorPlane, options, None)
82 # EndBlock
83
84 # Delete Selection
85 selection = Selection.Create(Face1)
86 result = Delete.Execute(selection)
87
88
89
90 # Delete Selection
91 selection = Selection.Create(GetRootPart().DatumPlanes[0])
92 result = Delete.Execute(selection)
93 # EndBlock
94
95
96 # Set Sketch Plane
97 sectionPlane = Plane.PlaneXY
98 result = ViewHelper.SetSketchPlane(sectionPlane, None)
99 # EndBlock
100
101
102
103 # Sketch Rectangle
104 plane = Plane.PlaneXY
105 result = ViewHelper.SetSketchPlane(plane)
106 point1 = Point2D.Create(MM(-200),MM(0))
107 point2 = Point2D.Create(MM(1100),MM(0))
108 point3 = Point2D.Create(MM(1100),MM(800))
109 result = SketchRectangle.Create(point1, point2, point3)
110 # EndBlock
111
112
113 # Solidify Sketch
114 mode = InteractionMode.Solid
115 result = ViewHelper.SetViewMode(mode, None)
116 # EndBlock
117
118
119 # Set Sketch Plane
120 sectionPlane = Plane.PlaneXY
121 result = ViewHelper.SetSketchPlane(sectionPlane, None)
122 # EndBlock
```

```
123
124 # Sketch Rectangle
125 point1 = Point2D.Create(MM(-8000),MM(0))
126 point2 = Point2D.Create(MM(11000),MM(0))
127 point3 = Point2D.Create(MM(11000),MM(6000))
128 result = SketchRectangle.Create(point1, point2, point3)
129 # EndBlock
130
131 # Solidify Sketch
132 mode = InteractionMode.Solid
133 result = ViewHelper.SetViewMode(mode, None)
134 # EndBlock
135
136
137
138 # Set Sketch Plane
139 sectionPlane = Plane.PlaneXY
140 result = ViewHelper.SetSketchPlane(sectionPlane, None)
141 # EndBlock
142
143
144 # Sketch Rectangle
145 plane = Plane.PlaneXY
146 result = ViewHelper.SetSketchPlane(plane)
147 point1 = Point2D.Create(MM(1100),MM(800))
148 point2 = Point2D.Create(MM(11000),MM(800))
149 point3 = Point2D.Create(MM(11000),MM(6000))
150 result = SketchRectangle.Create(point1, point2, point3)
151 # EndBlock
152
153 # Sketch Rectangle
154 point1 = Point2D.Create(MM(-200),MM(800))
155 point2 = Point2D.Create(MM(-8000),MM(800))
156 point3 = Point2D.Create(MM(-8000),MM(6000))
157 result = SketchRectangle.Create(point1, point2, point3)
158 # EndBlock
159
160 # Solidify Sketch
161 mode = InteractionMode.Solid
162 result = ViewHelper.SetViewMode(mode, None)
163 # EndBlock
164
165 # Delete Selection
166 selection = Selection.Create(GetRootPart().Bodies[0].Faces[0])
167 result = Delete.Execute(selection)
168 # EndBlock
169
```

```
170 # Rest of script can be found with link below.
171 # https://drive.google.com/open?id=1
    IuBtu3fXVH75Bv30fat7QCT4EDOrWa7P
```

References

[1] B. Gilbert and K. Foreman, "Experiments with a diffuser-augmented model wind turbine," *Journal of Energy Resources Technology*, vol. 105, no. 1, pp. 46–53, 1983.

[2] O. Igra, "Research and development for shrouded wind turbines," *Energy Conversion and Management*, vol. 21, no. 1, pp. 13–48, 1981.

[3] D. Phillips, P. Richards, and R. Flay, "Cfd modelling and the development of the diffuser augmented wind turbine," *Wind and Structures*, vol. 5, no. 2_3_4, pp. 267–276, 2002.

[4] K.-i. Abe and Y. Ohya, "An investigation of flow fields around flanged diffusers using cfd," *Journal of wind engineering and industrial aerodynamics*, vol. 92, no. 3-4, pp. 315–330, 2004.

[5] M. O. L. Hansen, N. N. Sørensen, and R. Flay, "Effect of placing a diffuser around a wind turbine," *Wind Energy: An International Journal for Progress and Applications in Wind Power Conversion Technology*, vol. 3, no. 4, pp. 207–213, 2000.

[6] D. Hartwanger and A. Horvat, "3d modelling of a wind turbine using cfd," in *NAFEMS Conference, United Kingdom*, 2008.

[7] E. Duque, C. Van Dam, and S. Hughes, "Navier-stokes simulations of the nrel combined experiment phase ii rotor," in *37th Aerospace Sciences Meeting and Exhibit*, 1999, p. 37.

[8] U. Saha, S. Thotla, and D. Maity, "Optimum design configuration of savonius rotor through wind tunnel experiments," *Journal of Wind Engineering and Industrial Aerodynamics*, vol. 96, no. 8-9, pp. 1359–1375, 2008.

[9] B. D. Altan and M. Atılgan, "An experimental and numerical study on the improvement of the performance of savonius wind rotor," *Energy Conversion and Management*, vol. 49, no. 12, pp. 3425–3432, 2008.

[10] R. Wu, Y. Chen, Y. Pan, Q. Wang, and D. Zhang, "Determination of three-dimensional movement for rotary blades using digital image correlation," *Optics and Lasers in Engineering*, vol. 65, pp. 38–45, 2015.

[11] J. Winstroth, L. Schoen, B. Ernst, and J. R. Seume, "Wind turbine rotor blade monitoring using digital image correlation: A comparison to aeroelastic simulations of a multi-megawatt wind turbine," in *Journal of Physics: Conference Series*, IOP Publishing, vol. 524, 2014, p. 012 064.

[12] F. Kelberlau, "Free decay testing of a semisubmersible offshore floating platform for wind turbines in model scale," 2017.

[13] F. R. Menter, M. Kuntz, and R. Langtry, "Ten years of industrial experience with the sst turbulence model," *Turbulence, heat and mass transfer*, vol. 4, no. 1, pp. 625–632, 2003.

[14] N. Mandas, F. Cambuli, and C. E. Carcangiu, "Numerical prediction of horizontal axis wind turbine flow," *University of Caglairi, EWEC*, 2006.

[15] P. Fuglsang and H. A. Madsen, "Optimization method for wind turbine rotors," *Journal of Wind Engineering and Industrial Aerodynamics*, vol. 80, no. 1-2, pp. 191–206, 1999.

[16] J. Li, R. Li, Y. Gao, and J. Huang, "Aerodynamic optimization of wind turbine airfoils using response surface techniques," *Proceedings of the Institution of Mechanical Engineers, Part A: Journal of Power and Energy*, vol. 224, no. 6, pp. 827–838, 2010.

[17] P.-Å. Krogstad and M. S. Adaramola, "Performance and near wake measurements of a model horizontal axis wind turbine," *Wind Energy*, vol. 15, no. 5, pp. 743–756, 2012.

[18] GWEC, "Global wind report 2018," GWEC, Tech. Rep., 2019.

[19] "The inside of a wind turbine," *Energy.gov*, [Online]. Available: `https://www.energy.gov/eere/wind/inside-wind-turbine`.

[20] W. Schmidt and H. von Alexandria, *Heron von Alexandria*. Teubner, 1899.

[21] H. E. Wulff, "The traditional crafts of persia," 1966.

[22] S. Prout, *A view of a windmill with a small ladder placed by the doorway*, 1815.

[23] D. Wray, "European post-mill," [Online]. Available: `http://www.norfolkmills.co.uk/Library/Postmill-cutaway.jpg`.

[24] R. v. Rijn, "The windmill," 1641. [Online]. Available: `https://www.metmuseum.org/toah/works-of-art/41.1.12/`.

[25] D. A. De Maus, "Sailing ship chance aground at bluff," *National Library of New Zealand*, 1902. [Online]. Available: `https://natlib.govt.nz/records/22748045?search[il][category]=Images&search[path]=items&search[text]=chance%20aground`.

[26] T. J. Price, "James blyth—britain's first modern wind power pioneer," *Wind engineering*, vol. 29, no. 3, pp. 191–200, 2005.

[27] D. G. J. Marie, "Turbine having its rotating shaft transverse to the flow of the current," 1931, US Patent 1,835,018.

[28] G. Koeppl, "Putnam's power from the wind," Jan. 1982.

[29] NASA, "Wind generator of nasa," 1995. [Online]. Available: `http://www.windsofchange.dk/WOC-usastat.php`.

[30] Tvind, "The wind turbine at tvind," 1978. [Online]. Available: `https://www.tvindkraft.dk`.

[31] E. Lantz, M. Hand, and R. Wiser, "Past and future cost of wind energy," National Renewable Energy Lab.(NREL), Golden, CO (United States), Tech. Rep., 2012.

[32] W. Europe, "Wind energy in europe in 2018,trends and statistics," *https://windeurope.org/wp-content/uploads/files/about-wind/statistics/WindEurope-Annual-Statistics-2018.pdf*, 2019.

[33] A. Betz, “Wind energy and its exploitation by windmills,” *Gottingen: Vandenhoeck und Ruprccht*, vol. 64, 1926.

[34] ANSYS Inc., “ANSYS Fluent Theory Guide,” 2019.

Publications From the Thesis

Contact Information: safakdogr@gmail.com

Conference Papers

1. S. Doğru, O. Yılmaz, A. C. Koyuncuoglu, “Aerodynamic optimization of rotating diffuser for horizontal Axis Wind Turbine,”, 5th international conference on engineering and natural sciences,”, Prague, 2019.